

# Electrical Spectroscopy Studies of Lithium and Magnesium Polymer Electrolytes Based on PEG400

Vito Di Noto\*

Dipartimento di Chimica Inorganica, Metallorganica ed Analitica, Via Loredan 4, I-35131 Padova, Italy

Received: March 20, 2002

Four classes of solvent-free polymer electrolytes were prepared in order to study the mechanism of ionic motion and the interactions existing in polymer electrolytes. The following electrolytic complexes were studied PEG400/(MgCl<sub>2</sub>)<sub>x</sub> (0.00329 ≤ *x* ≤ 0.7000) (PEG400 = poly(ethylene glycol) 400); poly[PEG400-*alt*-DEOS]/(MgCl<sub>2</sub>)<sub>x</sub> (6.28 × 10<sup>-2</sup> ≤ *x* ≤ 13.16) (DEOS = diethoxydimethylsilane); [EDTA][PEG400]<sub>2</sub>/(LiCl)<sub>2.26</sub>; [EDTA]-[PEG400]<sub>2</sub>/(MgCl<sub>2</sub>)<sub>1.98</sub>; [EDTA][PEG400]<sub>2</sub>/(LiCl)<sub>2.26</sub>(MgCl<sub>2</sub>)<sub>1.9</sub>; [EDTA]<sub>3</sub>[PEG400]<sub>7</sub>/(LiCl)<sub>6.39</sub>; [EDTA]<sub>3</sub>-[PEG400]<sub>7</sub>/(MgCl<sub>2</sub>)<sub>8.23</sub>; and [EDTA]<sub>3</sub>[PEG400]<sub>7</sub>/(LiCl)<sub>6.39</sub>(MgCl<sub>2</sub>)<sub>6.16</sub> (EDTA = ethylenediaminetetraacetic acid). The studies were carried out by impedance spectroscopy in the 20 Hz to 1 MHz range at different temperatures. Real and imaginary components of conductivity spectra in terms of equivalent circuit analysis and correlated ionic motion analysis based on a generalized universal power law were investigated. Results revealed that in the PEG400/(MgCl<sub>2</sub>)<sub>x</sub> and poly[PEG400-*alt*-DEOS]/(MgCl<sub>2</sub>)<sub>x</sub> systems the ionic species formed in the bulk materials are crucial for the overall conductivity. Indeed, in PEG400/(MgCl<sub>2</sub>)<sub>x</sub>, conductivity takes place through hopping of the cationic species Mg<sup>2+</sup> and [MgCl]<sup>+</sup> between the coordination sites present along the polyether chains. In poly[PEG400-*alt*-DEOS]/(MgCl<sub>2</sub>)<sub>x</sub> systems, two types of mechanisms were detected: (a) the migration of cationic species Mg<sup>2+</sup> and [MgCl]<sup>+</sup> at low salt concentrations and (b) the hopping of Cl<sup>-</sup> anions between magnesium species coordinated by the oxygen donor atoms of polyether chains at high salt concentrations. This latter phenomenon results in cation migration without any substantial geometric site relaxation. Studies of the lithium and magnesium polymer electrolytes based on [EDTA]-[PEG400]<sub>2</sub> and [EDTA]<sub>3</sub>[PEG400]<sub>7</sub> polymers revealed that the type and geometry of coordination sites present in the polymer host are of crucial importance in modulating the conductivity of the polymer electrolytes. In particular, the chelating EDTA sites, which are able to strongly coordinate cations such as Mg<sup>2+</sup>, are excluded from the overall conductivity mechanism.

## 1. Introduction

Polymer electrolytes (PE) are crucial materials for the development of modern electronic devices such as high energy-density batteries, sensors, fuel cells, electrochromic displays, etc.<sup>1–4</sup> The classical polymer electrolytes consist of organic macromolecules (usually polyether polymers) that are doped with inorganic salts<sup>1</sup>. It was demonstrated that ion transport in these materials occurs through amorphous polymer electrolyte region phases.<sup>1</sup> Ionic conductivity in polyether-based solid polymer electrolytes is low at room temperature.<sup>1,2,5–9</sup> Indeed, in general, a conductivity ranging from 10<sup>-3</sup> to 10<sup>-4</sup> S cm<sup>-1</sup> is observed at 100 °C, whereas at room-temperature, values in the 10<sup>-6</sup>–10<sup>-8</sup> S cm<sup>-1</sup> range are measured. Several investigators suggested that conductivity in these systems occurs through two phenomena.<sup>10–12</sup> The first is associated with the charge migration of ions between coordination sites in the host material, and the second is attributed to the increase in conductivity observed as a result of polymeric chain motions, the so-called “segmental-motion”.<sup>1</sup> Theoretical models have been proposed to explain the mechanism responsible for ionic conductivity in these systems, and molecular dynamic (MD) and Monte Carlo (MC) simulations have been carried out for crystalline and amorphous poly(ethylene oxide) (PEO) and PEO/salt complexes.<sup>13–18</sup>

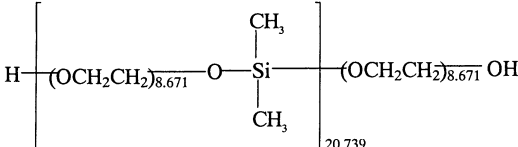
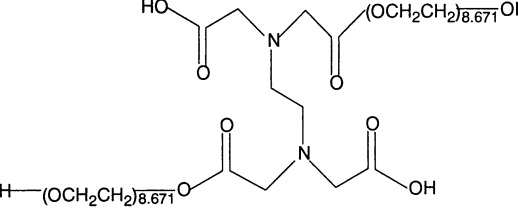
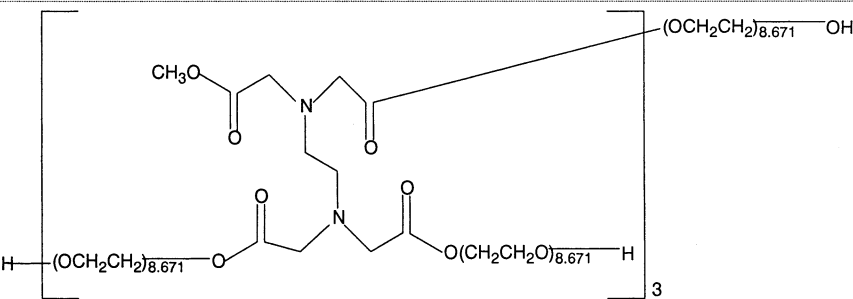
Ratner et al.<sup>11,12,19,20</sup> developed a dynamic bond percolation theory that explains the charge migration in the system in terms of the renewal of hopping probabilities. Through a combination of theoretical modeling and accurate experimental studies, Furukawa et al.<sup>21</sup> reported accurate measurements of complex conductivity spectra for polypropylene oxide PPO/(LiClO<sub>4</sub>)<sub>x</sub> complexes. These authors proposed that conductivity takes place through two phenomena.<sup>21,22</sup> The first of these, which is detected at high frequencies, is associated with dielectric relaxations due to dipolar motions caused by the segmental and normal-mode dynamics of the polymer host; the second, which is observed at lower frequencies, is attributed to local ionic motions. It was also demonstrated that conductance of a variety of polymer electrolyte complexes increases up to a maximum with increasing salt concentrations and then decreases at high salt concentrations.<sup>23,24</sup>

The aim of this study was to obtain further experimental evidence in order to understand the connections between the macroscopic conductivity and the microscopic molecular events involved in the conductivity mechanisms in terms of ionic species, coordination sites in polymer hosts, and polymer segmental motion.

To carry out these investigations, we prepared extremely anhydrous polymer electrolytes based on PEG400 polyether chains. In particular, the influence of host polymer mobility and chemically different coordination sites on the overall conductivity

\* To whom correspondence should be addressed. E-mail: vito.dinoto@unipd.it.

## SCHEME 1: Structures of the Host Polymers Used for the Preparation of Polymer Electrolytes

Structure	Polymer
a) $\text{H}(\text{OCH}_2\text{CH}_2)_{8.671}\text{OH}$	PEG400
b)  $M_w=9860 \text{ g/mol}$	poly[PEG400-alt-DEOS]/(MgCl <sub>2</sub> ) <sub>x</sub>
c)  $M_w=1095 \text{ g/mol}$	[EDTA][PEG400] <sub>2</sub>
d)  $M_w=3702 \text{ g/mol}$	[EDTA] <sub>3</sub> [PEG400] <sub>7</sub>

ity was investigated by collecting accurate impedance spectroscopy measurements on polymer electrolytes based on four types of host polymers and two types of salts. Poly(ethylene glycol) 400 (PEG400), poly[PEG400-*alt*-DEOS] (DEOS = diethoxydimethylsilane), [EDTA][PEG400]<sub>2</sub>, and [EDTA]<sub>3</sub>[PEG400]<sub>7</sub> were used as host polymers in the preparation of polymer electrolytes (EDTA = ethylenediaminetetraacetic acid). The first two host polymers were chosen because they offer the well-known coordination sites present in the polyether polymer electrolytes;<sup>23,25</sup> the second two were examined because they in addition present two different types of chelating sites based on EDTA moieties<sup>26,27</sup> of the chain polymer.

Lithium chloride<sup>25</sup> and  $\delta$ -MgCl<sub>2</sub><sup>28</sup> were used as salts. These individual salts and mixtures of both were used in order to study the effect of site coordination selectivity on the overall conductivity of the prepared polymer electrolytes. Therefore, the host polymers were used to prepare polymer electrolytes doped with lithium chloride, magnesium chloride, and mixtures of both. The spectrum of the real component of the conductivity measurements was interpreted in terms of ion hopping and host medium reorganization on the basis of the theoretical results of the dynamic disorder hopping models previously proposed.<sup>19,20,29–32</sup> The equivalent conductivity in relation to temperature and composition was also investigated.

A complete interpretation of the electrical spectroscopic data was achieved by adopting a combined approach based on a generalized universal power law<sup>8,33–35</sup> (UPL) in the framework of the jump–relaxation model<sup>34–36</sup> and on an analysis in terms of equivalent circuits.<sup>37</sup> The correlation of the results described here with the available structural information for the investigated systems allowed the proposal of plausible conductivity mech-

anisms for the polymer electrolytes and revealed the influence of the coordination capability and selectivity of sites based on EDTA chelating units and polyether oxygen atoms on the overall conductivity of the investigated systems.

## 2. Experimental Section

**2.1. Materials.**  $\delta$ -MgCl<sub>2</sub> and LiCl were prepared as reported in refs 38 and 25, respectively. PEG 400 and solvents were supplied by Aldrich and further purified by standard methods. Poly[PEG400-*alt*-DEOS] was prepared as reported in ref 39, and [EDTA][PEG400]<sub>2</sub> and [EDTA]<sub>3</sub>[PEG400]<sub>7</sub> were prepared according to the procedure described in ref 40. The structures of the host polymers are shown together with their molecular weights in Scheme 1. PEG400/(MgCl<sub>2</sub>)<sub>x</sub> polymer electrolytes with  $0.00329 \leq x \leq 0.7000$  were synthesized as described in ref 38. Poly[PEG400-*alt*-DEOS]/(MgCl<sub>2</sub>)<sub>x</sub> with  $6.28 \times 10^{-2} \leq x \leq 13.16$  were prepared following the protocol described in ref 39. The complexes based on [EDTA][PEG400]<sub>2</sub> and [EDTA]<sub>3</sub>[PEG400]<sub>7</sub> were synthesized according to ref 40. The compositional details and physical properties of these compounds are summarized in Table 1 and Scheme 2.

**2.2. Instrumentation.** AC impedance measurements were performed between 20 Hz and 1 MHz by means of a computer-controlled HP4284A precision LCR meter. The 4-terminal pair measurement method was adopted using two types of homemade Teflon cells. The sample in the form of film was placed between two cylindrical gold-plated stainless steel electrodes. One electrode was guarded, and the other was unguarded. In the first cell the diameter of the unguarded electrode was 56 mm and that of guarded electrode 38 mm. The gap between guarded and guard electrode was 0.2 mm. In the second cell, the diameter

TABLE 1: Compositional Data for Investigated Polymer Electrolytes

(a) <sup>a</sup>					
PEG400/(MgCl <sub>2</sub> ) <sub>x</sub>			poly[PEG400- <i>alt</i> -DEOS]/(MgCl <sub>2</sub> ) <sub>x</sub>		
<i>x</i>	<i>m</i>	Mg/O	<i>x</i>	<i>m</i>	Mg/O
7.00 × 10 <sup>-1</sup>	1.749	7.23 × 10 <sup>-2</sup>	13.16	1.184	5.55 × 10 <sup>-2</sup>
3.04 × 10 <sup>-1</sup>	0.760	3.15 × 10 <sup>-2</sup>	7.686	0.726	3.40 × 10 <sup>-2</sup>
1.20 × 10 <sup>-1</sup>	0.281	1.16 × 10 <sup>-2</sup>	1.984	0.197	9.26 × 10 <sup>-3</sup>
1.02 × 10 <sup>-1</sup>	0.254	1.05 × 10 <sup>-2</sup>	6.44 × 10 <sup>-1</sup>	0.065	3.04 × 10 <sup>-3</sup>
5.18 × 10 <sup>-2</sup>	0.129	5.36 × 10 <sup>-3</sup>	2.60 × 10 <sup>-1</sup>	0.026	1.23 × 10 <sup>-3</sup>
2.33 × 10 <sup>-2</sup>	0.058	2.24 × 10 <sup>-3</sup>	1.38 × 10 <sup>-1</sup>	0.014	6.56 × 10 <sup>-4</sup>
1.04 × 10 <sup>-2</sup>	0.026	1.08 × 10 <sup>-3</sup>	6.28 × 10 <sup>-2</sup>	0.006	2.99 × 10 <sup>-4</sup>
3.29 × 10 <sup>-3</sup>	0.008	3.31 × 10 <sup>-4</sup>			
(b) <sup>b</sup>					
complex	<i>x</i>	<i>y</i>	<i>m<sub>x</sub></i>	<i>m<sub>y</sub></i>	M/O
[EDTA][PEG400] <sub>2</sub> /(LiCl) <sub>x</sub>	2.26	-	2.066		0.08920
[EDTA][PEG400] <sub>2</sub> /(MgCl <sub>2</sub> ) <sub>y</sub>		1.98		1.806	0.07815
[EDTA][PEG400] <sub>2</sub> /(LiCl) <sub>x</sub> (MgCl <sub>2</sub> ) <sub>y</sub>	2.26	1.9	1.899	1.732	0.0892 <sup>c</sup> + 0.07499 <sup>d</sup> = 0.16419
[EDTA] <sub>3</sub> [PEG400] <sub>7</sub> /(LiCl) <sub>x</sub>	6.39		1.727		0.07728
[EDTA] <sub>3</sub> [PEG400] <sub>7</sub> /(MgCl <sub>2</sub> ) <sub>y</sub>		8.23		2.225	0.09954
[EDTA] <sub>3</sub> [PEG400] <sub>7</sub> /(LiCl) <sub>x</sub> (MgCl <sub>2</sub> ) <sub>y</sub>	6.39	6.16	1.745	1.6830	0.07728 <sup>c</sup> + 0.07451 <sup>d</sup> = 0.15179

<sup>a</sup> *x* = mol<sub>MgCl<sub>2</sub></sub>/mol<sub>polymer</sub>; *m* = mol<sub>MgCl<sub>2</sub></sub>/kg<sub>polymer</sub>; Mg/O = molar ratio *n<sub>Mg</sub>*/*n<sub>O</sub>*. <sup>b</sup> *x* = mol<sub>LiCl</sub>/mol<sub>polymer</sub>; *y* = mol<sub>MgCl<sub>2</sub></sub>/mol<sub>polymer</sub>; *m<sub>x</sub>* = mol<sub>LiCl</sub>/kg<sub>polymer</sub>; *m<sub>y</sub>* = mol<sub>MgCl<sub>2</sub></sub>/kg<sub>polymer</sub>; M/O = *n<sub>metal ions</sub>*/*n<sub>O</sub>*. <sup>c</sup> Li/O molar ratio. <sup>d</sup> Mg/O molar ratio.

SCHEME 2: Composition and Physical Consistencies of the Investigated Polymer Electrolytes

Complex		Physical Status
(I)	PEG400/(MgCl <sub>2</sub> ) <sub>x</sub> with 3.29·10 <sup>-3</sup> ≤ <i>x</i> ≤ 0.7	highly viscous liquids
(II)	poly[PEG400- <i>alt</i> -DEOS]/(MgCl <sub>2</sub> ) <sub>x</sub> with 6.284·10 <sup>-2</sup> ≤ <i>x</i> ≤ 13.16	highly viscous liquids
(III)	[EDTA][PEG400] <sub>2</sub> /(LiCl) <sub>2.26</sub>	highly viscous liquid
(IV)	[EDTA][PEG400] <sub>2</sub> /(MgCl <sub>2</sub> ) <sub>1.98</sub>	solid powder
(V)	[EDTA][PEG400] <sub>2</sub> /(LiCl) <sub>2.26</sub> (MgCl <sub>2</sub> ) <sub>1.98</sub>	solid powder
(VI)	[EDTA] <sub>3</sub> [PEG400] <sub>7</sub> /(LiCl) <sub>6.39</sub>	highly viscous liquid
(VII)	[EDTA] <sub>3</sub> [PEG400] <sub>7</sub> /(MgCl <sub>2</sub> ) <sub>8.23</sub>	gummy material
(VIII)	[EDTA] <sub>3</sub> [PEG400] <sub>7</sub> /(LiCl) <sub>6.39</sub> (MgCl <sub>2</sub> ) <sub>6.16</sub>	gummy material

of the unguarded electrode was 20 mm and that of guarded electrode 5 mm. The gap between guard and guarded electrode was 0.13 mm. In both cells, the internal cylindrical guarded electrode was coaxial with the external guard electrode and isolated by Teflon rings. The sample thickness was measured using a micrometer. No corrections for thermal expansion of the cell were carried out. For liquid samples, a constant sample thickness has been ensured by fused silica fiber spacers with diameters in the range 125–500 μm. The cell containing the sample was prepared and enclosed in a glass tube in an argon drybox. The temperature of the sample was measured by a thermocouple inserted into the body of the guarded electrode (cell input) and controlled by immersion of the glass tube in a thermostatic silicon bath inserted into a Faraday cage. About 1 h was required between each temperature run to obtain equilibrium conditions. The temperature was measured with an accuracy greater than ±0.1 °C. Each impedance value was obtained by averaging five measurements at the same frequency. In dependence on the sample resistance, excitation amplitudes in the range 0.5–0.1 V were adopted. All of the frequency points of HP4284A precision LCR meter were measured (587 data points). Conductivity data were determined from complex impedance measurements using the “equivalent circuit” software package developed by Boukamp<sup>41</sup> and the

equivalent circuit model reported in ref 38. The calculated resistance values were affected by an error of less than 2%.

### 3. Results and Discussion

**3.1. Structural Characteristics and Properties of the Investigated PE.** This report was devoted to the study of the conducting properties of a number of chemically different PE systems (Schemes 1 and 2). It is to be underlined that all these materials are based on polyether PEG400 chains in order to obtain complexes with the degree of chain flexibility, cation complexation, and ion-pair separation capabilities which are typical properties of polyether chains.<sup>23,25</sup> In the poly[PEG400-*alt*-DEOS] polymer, bonding of the PEG400 units through very flexible dimethylsiloxane bridges confers the structural characteristics of PEG400 to a high molecular weight polymer (i.e., poly[PEG400-*alt*-DEOS], MW 9860 g/mol), having a very low concentration of OH groups.<sup>39</sup>

[EDTA][PEG400]<sub>2</sub> and [EDTA]<sub>3</sub>[PEG400]<sub>7</sub> are two polymers in which PEG400 units are bonded together through flexible EDTA bridges.<sup>40</sup> [EDTA][PEG400]<sub>2</sub> consists of linear chains which are more likely to be packed closely to one another compared to the chains in [EDTA]<sub>3</sub>[PEG400]<sub>7</sub>, where greater steric hindrance is expected.<sup>40</sup>

The polymer electrolytes prepared with the above-described host polymers are summarized in Scheme 2. The details of their compositions are reported in Table 1. The use of polymers with chelating sites allowed preparation of PE materials doped with mixtures of LiCl and  $\delta$ -MgCl<sub>2</sub> salts in order to study the effect of the metal ion coordination selectivity on the overall conductivity.

The physical consistencies of these materials are summarized in Scheme 2.

It was demonstrated that PEG400/(MgCl<sub>2</sub>)<sub>x</sub> polymers with  $x \leq 0.120$  consist of PEG400 TGT chains coordinating Mg<sup>2+</sup> ions by the polyether oxygens and Cl<sup>-</sup> anions by the terminal hydroxyls.

In addition, for  $x > 0.120$ , [Mg-Cl]<sup>+</sup> cations are detected in the bulk material.<sup>42</sup>

It was proposed that different ion species are present in poly-[PEG400-*alt*-DEOS]/(MgCl<sub>2</sub>)<sub>x</sub> PEs as  $x$  increases.<sup>39</sup> Specifically,<sup>42</sup> for  $x \leq 0.26$ , Mg<sup>2+</sup> is preferentially coordinated by polyether oxygen atoms and Cl<sup>-</sup> anions by the terminal hydroxyls of polymer chains; for  $0.26 < x \leq 1.984$ , [Mg-Cl]<sup>+</sup> cations in the bulk material are coordinated to both ether and terminal hydroxyl oxygens, and for  $x > 1.984$ , solvent separated triple ions of the types Cl<sup>-</sup>····[Mg-Cl]<sup>+</sup> and neutral species of the type MgCl<sub>2</sub> coordinated to polyether oxygen atoms are revealed in the bulk material. The main structural features of the polymer electrolytes based on [EDTA][PEG400]<sub>2</sub> and [EDTA]<sub>3</sub>[PEG400]<sub>7</sub> are as follows:<sup>40</sup> (a) the TGT chains of the polyether moieties are bridged by the flexible EDTA groups; (b) the Mg<sup>2+</sup> cations are preferentially coordinated by the chelating sites of the EDTA units present along the chains; (c) Li<sup>+</sup> is coordinated by oxygen atoms of EDTA moieties and polyether chains; (d) lithium-doped complexes of both polymers are highly viscous liquids; (e) the complexes doped with MgCl<sub>2</sub> and based on [EDTA][PEG400]<sub>2</sub> are all solid materials, thus indicating that Mg<sup>2+</sup> cations in these polymers are involved in the interchain cross-linked coordination; (f) the systems containing Mg<sup>2+</sup> and based on the [EDTA]<sub>3</sub>[PEG400]<sub>7</sub> are gummy materials, thus indicating that the amount of coordination cross-links of Mg in these macromolecules is low owing to steric hindrance.

**3.2. Electrical Spectroscopy Studies.** To study the correlations between the structure and the conductivity mechanism and to reveal the influence of the coordination sites and ionic species present in the bulk materials on the overall conductivity of the electrolytic complexes, two strategies have been followed. At first, two groups of polymer electrolytes (see Table 1a and Scheme 2) based on MgCl<sub>2</sub> and basically characterized by the typical polyether cation coordination site that has already been thoroughly described in the literature<sup>23,25</sup> were studied as a function of temperature and composition. Subsequent analyses were focused on two other types of polymer electrolyte complexes. In addition to the typical polyether coordination sites, these latter materials present a chelating group for ions, constituted by two nitrogen and four oxygen donor atoms (see Schemes 1 and 2). The effect of site selectivity was studied by using lithium and magnesium salts (see Scheme 2). Figures 1 and 2 report selected Nyquist plots in the 20  $\rightleftharpoons$  80 °C temperature range and 20 Hz to 1 MHz frequency range for some of the PE materials reported in Scheme 2. Semicircular arcs at high frequencies could be identified for all of the samples. For the materials with low conductivity, these semicircles are incomplete at lower frequencies. Spikes are detected at low frequencies only for the PEG400/(MgCl<sub>2</sub>)<sub>x</sub> and [EDTA]<sub>3</sub>-[PEG400]<sub>7</sub>/(LiCl)<sub>x</sub> complexes. These measurements strongly

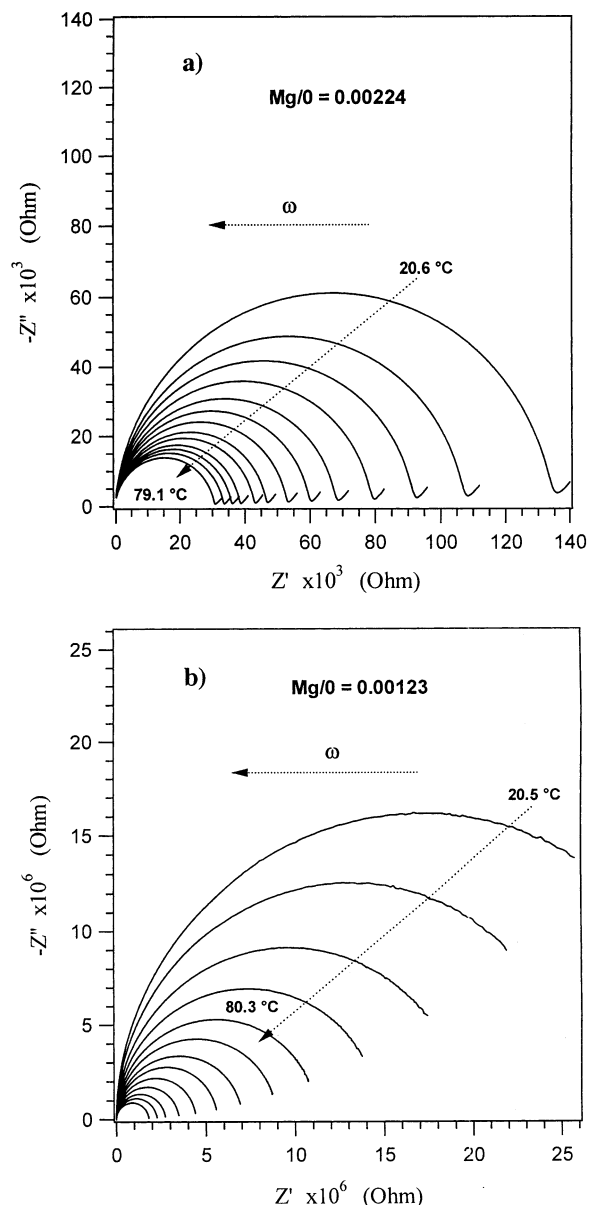


**Figure 1.** Nyquist plots of selected PEG400/(MgCl<sub>2</sub>)<sub>x</sub> (a) and poly-[PEG400-*alt*-DEOS]/(MgCl<sub>2</sub>)<sub>x</sub> complexes (b) at various temperatures. The measurements were carried out from 20 Hz to 1 MHz.

indicate that the temperature, composition, and types of ion-ion and ion-polymer interactions influence the frequency range and the shape of the Nyquist profiles. The single semicircle, easily identified in all of the materials, was simulated by using an equivalent circuit (EC) consisting of a geometrical capacitance in parallel with a bulk resistance. In the cases where spikes were observed at low frequencies, a constant phase element (CPE) was added in series to the parallel circuit described above.<sup>43</sup> In these latter conditions, fitting results indicated that the CPE elements are similar to the Warburg diffusion-limited impedances. Indeed, at all temperatures and compositions, the  $n$  parameter of the CPE element approximated to 0.5. On the other hand, the cell capacitances were found to be independent of concentration and temperature. In particular, cell capacitance values of ca.  $1.4 \times 10^{-10}$  and ca.  $1.25 \times 10^{-10}$  F were determined for PEG400/(MgCl<sub>2</sub>)<sub>x</sub> and poly[PEG400-*alt*-DEOS]/(MgCl<sub>2</sub>)<sub>x</sub> complexes, respectively, whereas both PEs based on [EDTA][PEG400]<sub>2</sub> and [EDTA]<sub>3</sub>[PEG400]<sub>7</sub> exhibited a capacitance of ca.  $6.8 \times 10^{-10}$  F. These findings indicate that the main spectral changes evident in Figures 1 and 2 are associated



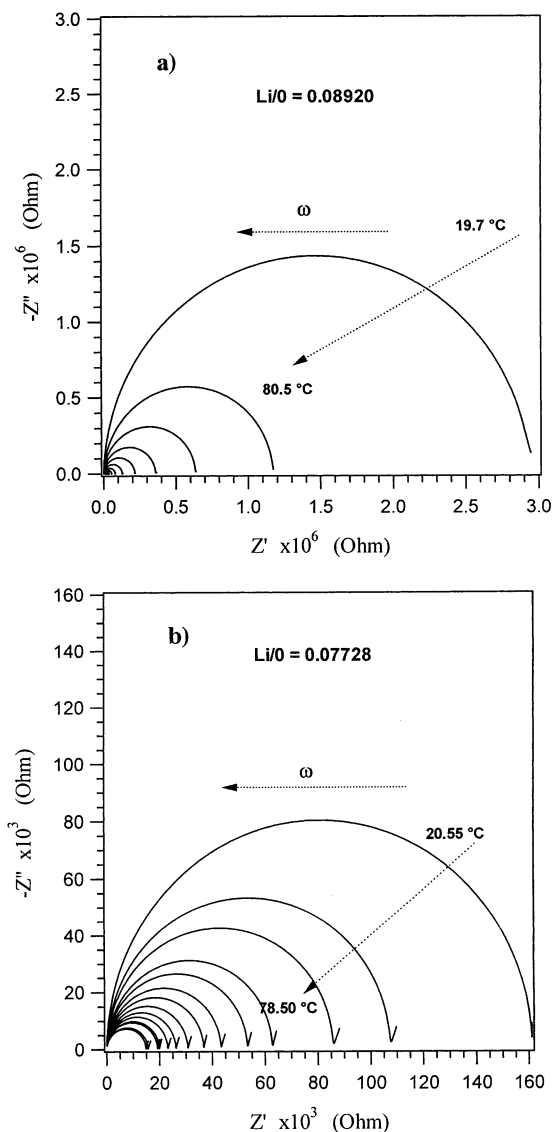


**Figure 2.** Nyquist plots of lithium polymer electrolytes based on [EDTA][PEG400]<sub>2</sub> (a) and [EDTA]<sub>3</sub>[PEG400]<sub>7</sub> polymers (b). The measurements were carried out from 20 Hz to 1 MHz.

with the resistance variation in the samples. The resulting bulk resistances were used to determine the conductivities of the PE complexes at different temperatures. EC data simulations were carried out using the EQUIVCRT program.<sup>41</sup> As demonstrated by Rolling<sup>32</sup> and confirmed in refs 8, 33, and 34, complete characterization of the AC electrical response of the studied systems required a detailed study of the real component of their conductivity.  $\sigma'(\omega)$  profiles were calculated as described in refs 8 and 34 by using the impedance data.  $\sigma'(\omega)$  spectra for some representative samples of the investigated systems are shown in Figures 3 and 4. In accordance with the investigations carried out on other polymer electrolytes,<sup>8,33,34</sup> these profiles are characterized by three different regions: (a) the low-frequency spike, (b) the medium-frequency plateau, and (c) the high-frequency spike. The low-frequency spikes correspond to the electrode polarization process, and the plateau is associated with the bulk conductivity of the PE materials. Indeed, both these regions are reproduced by using the equivalent circuit parameters ( $R$ ,  $C$ , and CPE element parameters) determined above with the EC method. On the other hand, the high-frequency portion of the  $\sigma'(\omega)$  curves depends on temperature and PE sample and cannot be reproduced by the equivalent circuit approach. All

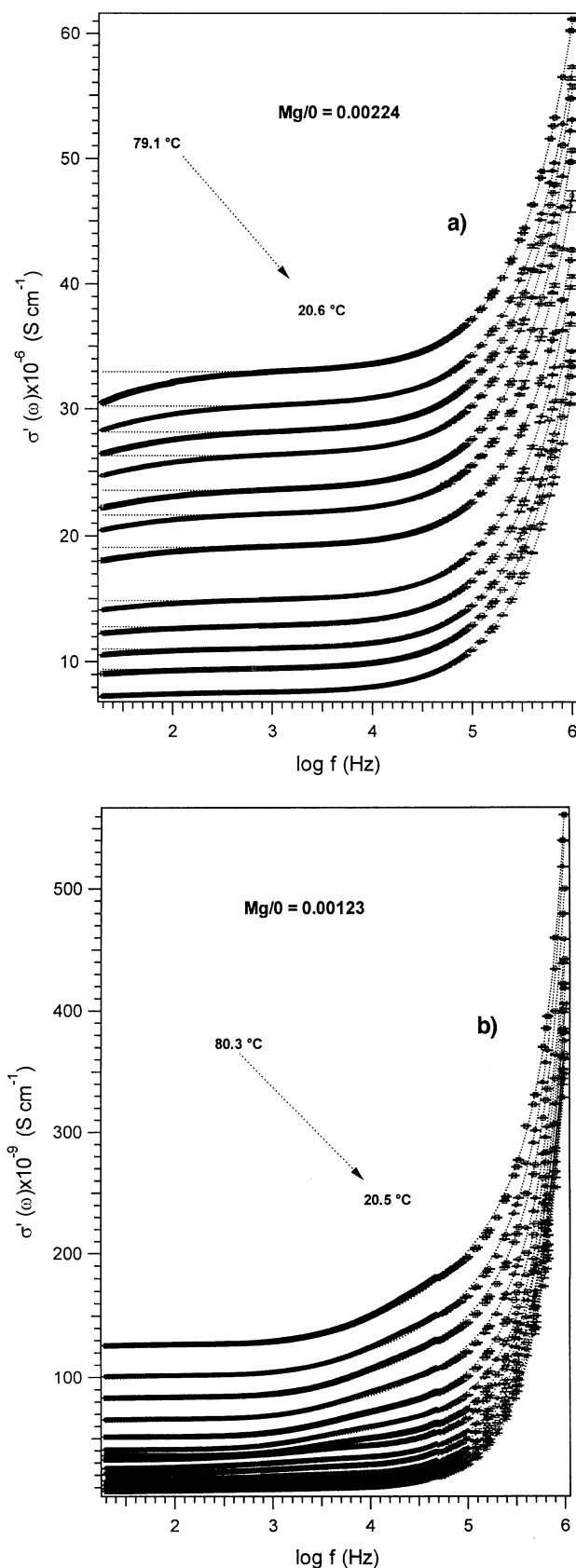


**Figure 3.** Real conductivity component,  $\sigma'(\omega)$ , versus  $\log f(\text{Hz})$  for selected PEG400/(MgCl<sub>2</sub>)<sub>x</sub> (a) and poly[PEG400-*alt*-DEOS]/(MgCl<sub>2</sub>)<sub>x</sub> complexes (b) measured at various temperatures. Dotted lines show the curves obtained by fitting  $\sigma'(\omega) = \sigma'(0)[1 + \sum_{i=1}^N f_i(\tau_{1,i}\omega)^{p_i}]$  to  $\sigma'(\omega)$  using experimental data obtained at frequencies higher than 1 kHz. The data were fitted using nonlinear least-squares procedures and  $N = 1$  for the PEG400/(MgCl<sub>2</sub>)<sub>x</sub> complexes (a) and  $N = 2$  for poly[PEG400-*alt*-DEOS]/(MgCl<sub>2</sub>)<sub>x</sub> (b).

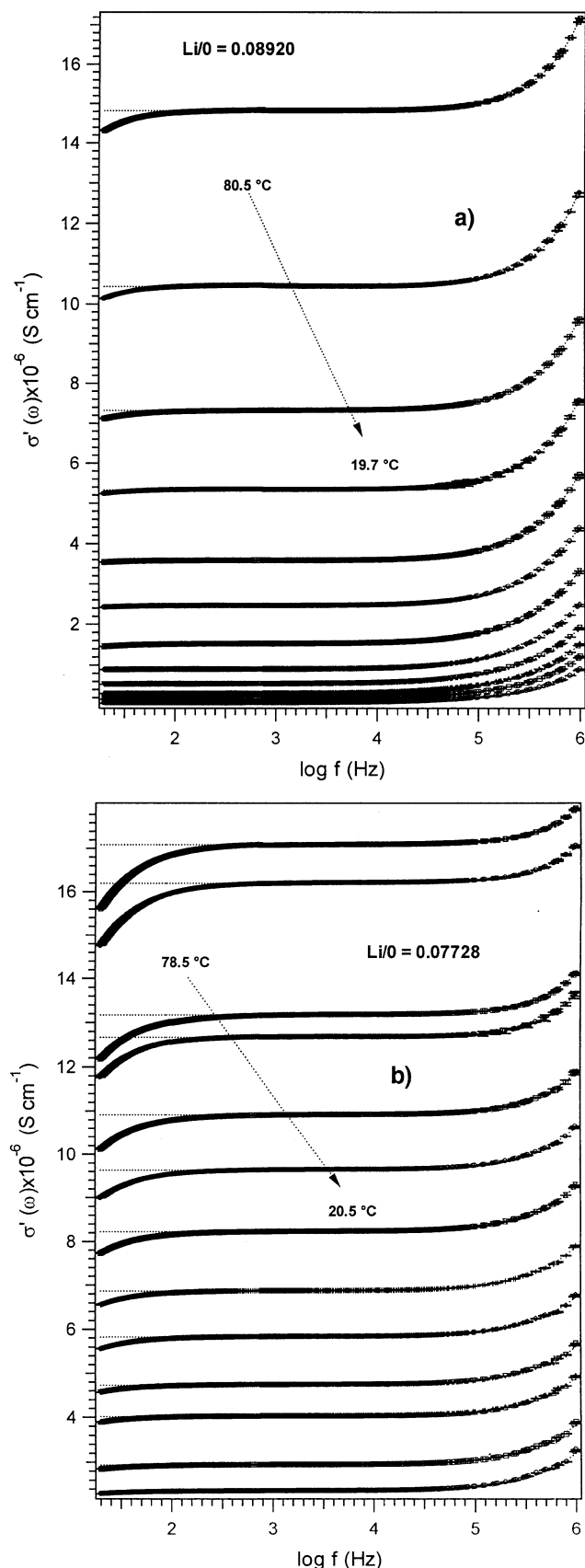


**Figure 4.** Real conductivity component,  $\sigma'(\omega)$ , versus  $\log f$  (Hz) for lithium polymer electrolytes based on [EDTA][PEG400]<sub>2</sub> (a) and [EDTA]<sub>3</sub>[PEG400]<sub>7</sub> polymers (b) measured at various temperatures. Dotted lines show the curves obtained by fitting  $\sigma'(\omega) = \sigma'(0)[1 + \sum_{i=1}^N f_i(\tau_{1,i}\omega)^{p_i}]$  to  $\sigma'(\omega)$  using experimental data obtained at frequencies higher than 1 kHz. The data were fitted using nonlinear least-squares procedures and  $N = 1$ .

of the investigated samples exhibit an increase in  $\sigma'(\omega)$  at high frequencies. This phenomenon is typical of systems in which correlated ionic motions in the PE bulk material are responsible for ionic conductivity.<sup>31–36,44,45</sup> A detailed analysis of the  $\sigma'(\omega)$  spectra (Figure 3 and 4) indicates that, with the exception of the poly[PEG400-*alt*-DEOS]/(MgCl<sub>2</sub>)<sub>x</sub> complexes, all of the materials exhibit a simple power law<sup>33–35</sup> behavior at frequencies higher than 1 kHz. Nevertheless, depending on the salt concentration, the  $\sigma'(\omega)$  spectra of the poly[PEG400-*alt*-DEOS]/(MgCl<sub>2</sub>)<sub>x</sub> systems (Figure 3b) disclose a further spectral feature at ca. 22 kHz which is superimposed on the overall power law profile. This additional spectral feature is typical of an additional correlated ionic motion process. On the basis of the results reported in the literature,<sup>32–34</sup> the analysis of correlated ionic motion in the framework of jump relaxation models could be carried out by fitting the  $\sigma'(\omega)$  data at frequencies higher than 1 kHz with the following generalized universal power law (G-UPL) equation:

$$\sigma'(\omega) = \sigma'(0)[1 + \sum_{i=1}^N f_i(\tau_{1,i}\omega)^{p_i}], \quad \text{with } \sum_{i=1}^N f_i = 1 \quad (1)$$

where  $\sigma'(0)$  denotes the DC conductivity ( $\sigma'(0) \cong \sigma_{\text{DC}}$ ). In accordance with Cramer et al.,<sup>45</sup>  $\tau_{1,i}$  is a time related to  $\tau_{2,i}$  ( $\tau_{1,i} = [(\sigma'(\infty) - \sigma'(0))/\sigma'(0)]^{1/p_i}\tau_{2,i}$ ), and  $\tau_{2,i}$  is the initial site relaxation time of ion hopping associated with the  $i$ th hopping process.  $p_i = \tau_{2,i}/\tau_i^*$  is the power law exponent and  $\tau_i^*$  is the initial back hop relaxation time.  $N$  indicates the number of processes, and  $f_i$  indicates the fractional contribution of the  $i$ th process to the overall conductivity. On the basis of refs 32–34, 45, and 46, the parameters of eq 1, which describe each charge migration process, can be physically interpreted as follows. For each ion in the bulk material, it is necessary to predict the existence of at least two types of coordination sites indicated as A and C (see Figure 5). If the ion hops from site A to site C, the effective potential minimum remains in A. Therefore, two distinct relaxation phenomena can occur. On one hand, the ion can hop back to A, giving no contribution to the overall conductivity. In this event, the effective potential of the sites remains unchanged<sup>44</sup> and the kinetics are regulated by the time constant  $\tau_i^*$ . On the other hand, to accommodate the ion in a coordination site characterized by a new absolute potential minimum, site C can relax with a kinetics regulated by  $\tau_{2,i}$  (the site relaxation time). It was suggested<sup>31–33,45</sup> that this latter process occurs through two distinct processes, i.e., a shift of the Coulomb cage and a geometrical relaxation caused by host network adjustment. In summary, the determination of the parameters  $p_i = \tau_{2,i}/\tau_i^*$  and  $\tau_{1,i}$  are of great importance in order to explain the overall conductivity in terms of ion migration processes in the materials. The polymer electrolytes investigated here, allowed a test of the applicability of eq 1 and a study of the possible correlations between the parameters of this equation and the different chemical sites and ionic species present in the bulk PE materials. Apart from the poly[PEG400-*alt*-DEOS]/(MgCl<sub>2</sub>)<sub>x</sub> systems, the investigated electrolytic complexes present molecular weights below the entanglement limit.<sup>47–50</sup> For simplicity, all of the sites present in the polymer chain containing a [polymer/M(x)-Cl]<sub>n</sub><sup>(x-n)+</sup> complex (with M being the metal ion,  $x$  its valence, and  $n$  the number of chloride coordinated to the metal,  $0 \leq n \leq 2$ ) can be designated as A sites and all of the coordination positions located along the axis of the empty polymer fragments surrounding the complex [polymer/M(x)-Cl]<sub>n</sub><sup>(x-n)+</sup> can be referred to as C sites. The hops between A sites do not require any substantial host medium

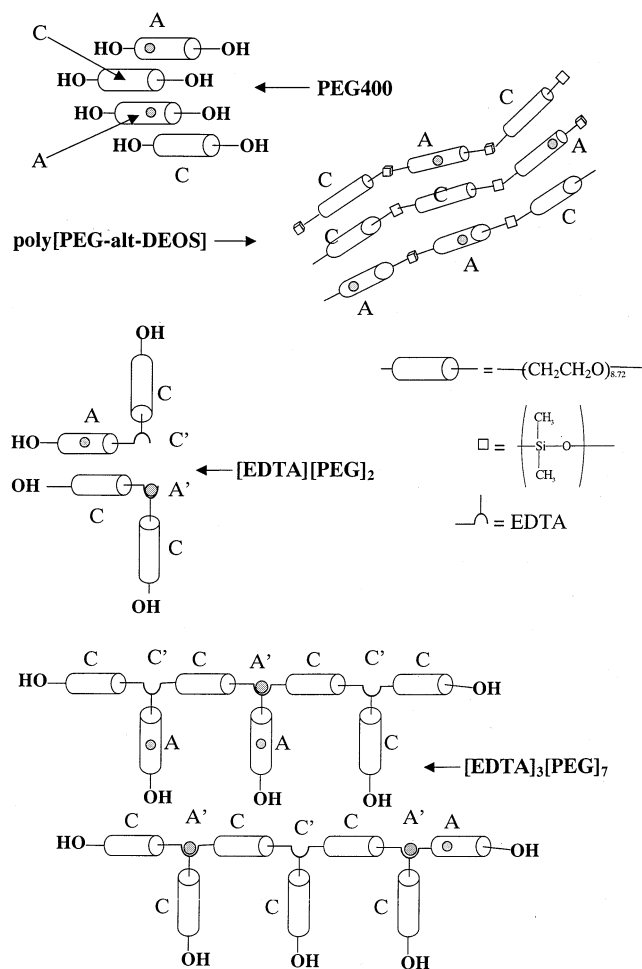


**Figure 5.** Schematic representation of the investigated PE materials. A and A' represent the sites coordinating a metal specie (full site), and C and C' are all of the other sites which could coordinate a metal ion specie (empty sites). A' and C' designate the sites present in the EDTA fragments.

reorganization. Interchain hopping events between A and C sites are expected to take place on two distinct time scale: the first associated with instantaneous hops and the second with the time involved in host medium reorganization.<sup>20,29,30</sup> Host medium reorganization processes can be attributed to two phenomena. The first event is associated with the ionic correlation events between the  $[\text{polymer}/\text{M}(x)\text{-Cl}_n]^{(x-n)+}$  complex cations and the  $\text{Cl}^-$  anions, and the second event is attributed to the geometrical reorganizations which occur after a hop in the coordination cage accommodating the ion. Depending on the valence of the metal and the salt concentration, two types of interchain hops could occur in the bulk material. The first event can be classified as cationic hopping ( $\alpha$ ) and the second as anionic hopping ( $\beta$ ). Both of these phenomena give rise to a cationic migration. The host medium reorganization events are expected to take place with ease if the polymer electrolyte is prepared using macromolecules below the entanglement regime or with polyether fragments bonded together by very flexible bridges. The curves represented by dotted lines in Figures 3a and 4 were obtained by fitting the experimental  $\sigma'(\omega)$  data with eq 1 at frequencies higher than 1 kHz and assuming  $N = 1$ . It should be pointed out that for the poly[PEG400-*alt*-DEOS]/( $\text{MgCl}_2$ )<sub>x</sub> polymer electrolytes (Figure 3b) it was necessary to use eq 1 with  $N = 2$ . Therefore, two types of ionic motion mechanisms were revealed in this material which were indicated as  $\alpha$  and  $\beta$  events. The dependence of the fractional contribution,  $f_2$ , of the  $\beta$

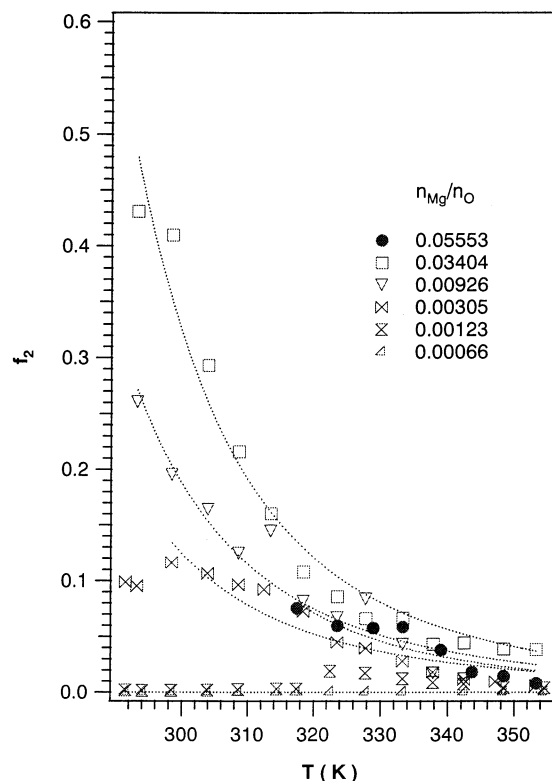


**Figure 6.** Dependence of parameter  $f_2$  on temperature for poly[PEG400-*alt*-DEOS]/( $\text{MgCl}_2$ )<sub>x</sub> complexes.  $f_2$  is the fractional contribution of  $\beta$  conduction process. It was obtained by fitting  $\sigma'(\omega) = \sigma'(0)[1 + \sum_{i=1}^N f_i(\tau_{1,i})^p]$  with  $N = 2$  to  $\sigma'(\omega)$  data.

charge-transfer process on temperature is shown in Figure 6. The influence of  $\beta$  on the overall conductivity decreases exponentially as the temperature increases, and the degree of its influence strongly depends on the composition of the poly[PEG400-*alt*-DEOS]/( $\text{MgCl}_2$ )<sub>x</sub> complex. Indeed, it is higher in the two electrolytic complexes having Mg/O molar ratios of 0.03404 and 0.00926.

Further confirmation<sup>34</sup> of the applicability of the G-UPL equation was obtained by plotting both  $\{\sigma'(\omega)\}/\{\sigma(0)\}$  and  $\ln[\sigma'(\omega)/\sigma(0) - 1]$  against logarithms of frequency.

For all temperatures and PE samples,  $\{\sigma'(\omega)\}/\{\sigma(0)\}$  exhibits a central plateau close to unity and a steep increase at high frequencies (Figure 7). The dependence on sample composition of the  $\{\sigma'(\omega)\}/\{\sigma(0)\}$  profiles (Figure 8) indicates that the high-frequency portion of  $\{\sigma'(\omega)\}/\{\sigma(0)\}$  spectra is diagnostic of material composition and charge-transfer mechanism. This representation and the fitting procedure described above lead one to predict a linear dependence of  $\ln[\sigma'(\omega)/\sigma(0) - 1]$  on  $\log(f/\text{Hz})$  at high frequencies for all of the spectra with the exception of those for the poly[PEG400-*alt*-DEOS]/( $\text{MgCl}_2$ )<sub>x</sub> complexes. On the other hand, if eq 1 holds with  $N = 2$ , a nonlinear dependence of the experimental  $\ln[\sigma'(\omega)/\sigma(0) - 1]$  on the  $\log(f/\text{Hz})$  is expected in the case of poly[PEG400-*alt*-DEOS]. All of these predictions were experimentally confirmed (see Figure 9). These observations, taken together with the applicability of the G-UPL dependence of the  $\sigma'(\omega)$  at high frequencies, demonstrates that the physical models for structurally disordered ionic conductors<sup>31–34,45</sup> are suitable for explaining the conductivity mechanism in the investigated polymer electrolytes. Furthermore, the plots of  $-Z(\omega)$  versus the logarithms of frequency revealed the presence of typical Debye peaks<sup>37</sup> (not shown). The frequency of the maxima in these Lorentzian profiles depends on the polymer electrolyte complex

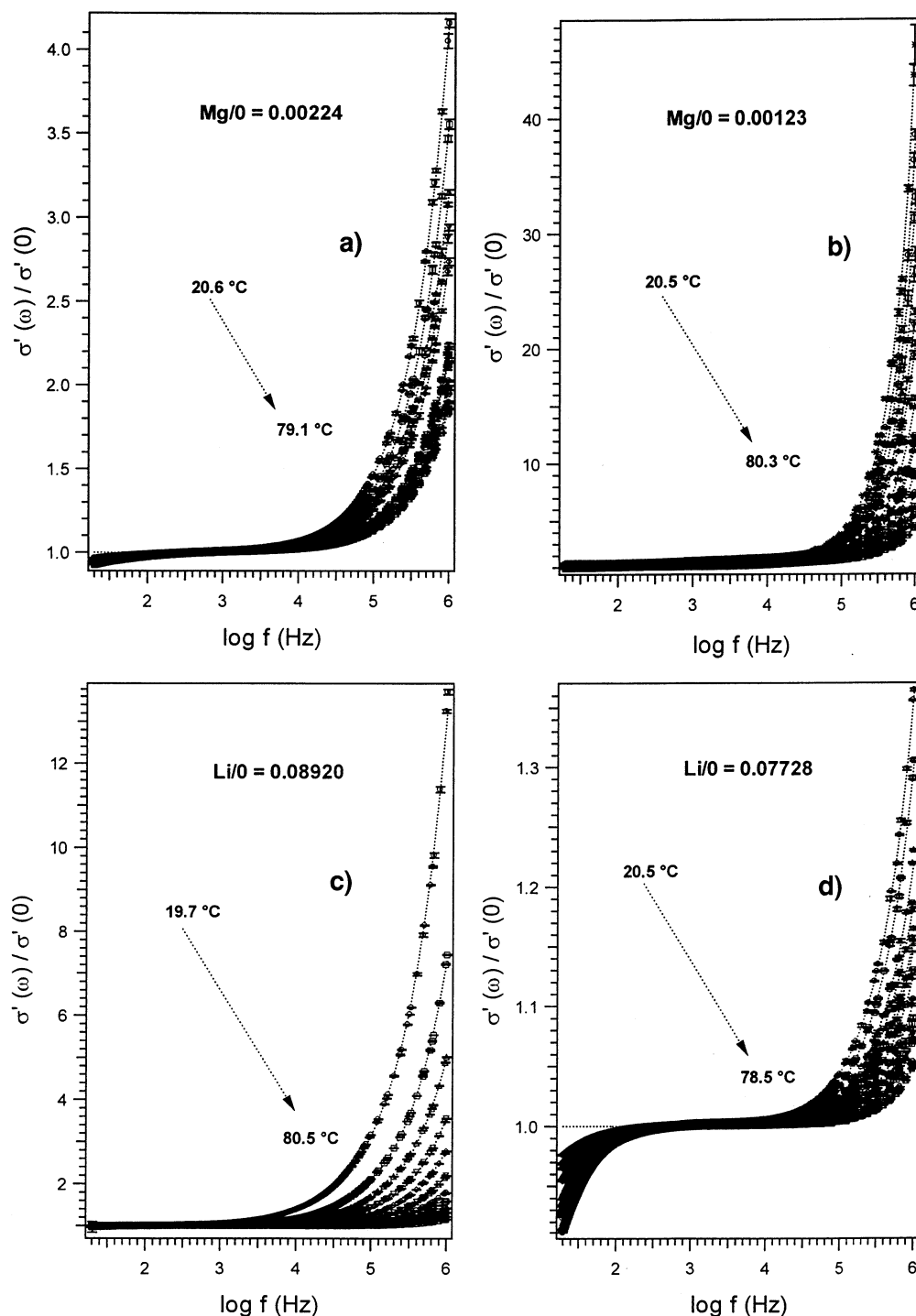


**Figure 7.**  $\{\sigma'(\omega)\}/\{\sigma'(0)\}$  as a function of  $\log f$  (Hz) for selected (a) PEG400/(MgCl<sub>2</sub>)<sub>x</sub>; (b) poly[PEG400-*alt*-DEOS]/(MgCl<sub>2</sub>)<sub>x</sub> complexes; lithium electrolytic complexes based on [EDTA][PEG400]<sub>2</sub> (c) and [EDTA]<sub>3</sub>[PEG400]<sub>7</sub> polymers (d). Simulated curves are shown by dotted lines.

and temperature. The conductivity relaxation times  $\tau_{\text{peak}} = 1/(f_{\text{peak}})$  ( $f_{\text{peak}}$  is the frequency of the maximum height of the peak) were determined by fitting the Debye peaks with Lorentzian functions.

To elucidate the conductivity mechanisms, the parameters determined by EC and G-UPL analysis were studied as a function of temperature and polymer electrolyte composition. The dependence of the logarithm of  $\sigma_{\text{EC}}(T)$  and  $\sigma'(0)$  on the reciprocal absolute temperature for the investigated PEs is shown in Figures 10 and 11. As expected, the values for  $\sigma_{\text{EC}}$  determined from the EC analysis are coincident with  $\sigma'(0)$  determined by fitting eq 1 to  $\sigma'(\omega)$  data at frequencies higher than 1 kHz. These results indicate that the conductivity value of the plateau of the

$\sigma'(\omega)$  profiles at frequencies higher than 1 kHz allow determination of the exact bulk conductivity of the material without any use of equivalent circuit analysis. Furthermore, the dependence of conductivity on temperature is reproduced by the empirical Vogel–Tamman–Fulcher<sup>11</sup> (VTF) law for PEG400/(MgCl<sub>2</sub>)<sub>x</sub> complexes and PEs based on [EDTA][PEG400]<sub>2</sub> and [EDTA]<sub>3</sub>[PEG400]<sub>7</sub> host polymers (see Figures 10a and 11).

The VTF equation is<sup>11</sup>

$$\sigma(T) = A_{\sigma} T^{-1/2} e^{-[E_{\sigma}]/[R(T-T_0)]} \quad (2)$$

where  $A_{\sigma}$  is proportional to the number of carrier ions,  $R$  is the gas constant,  $E_{\sigma}$  is the activation energy for conduction, and  $T_0$



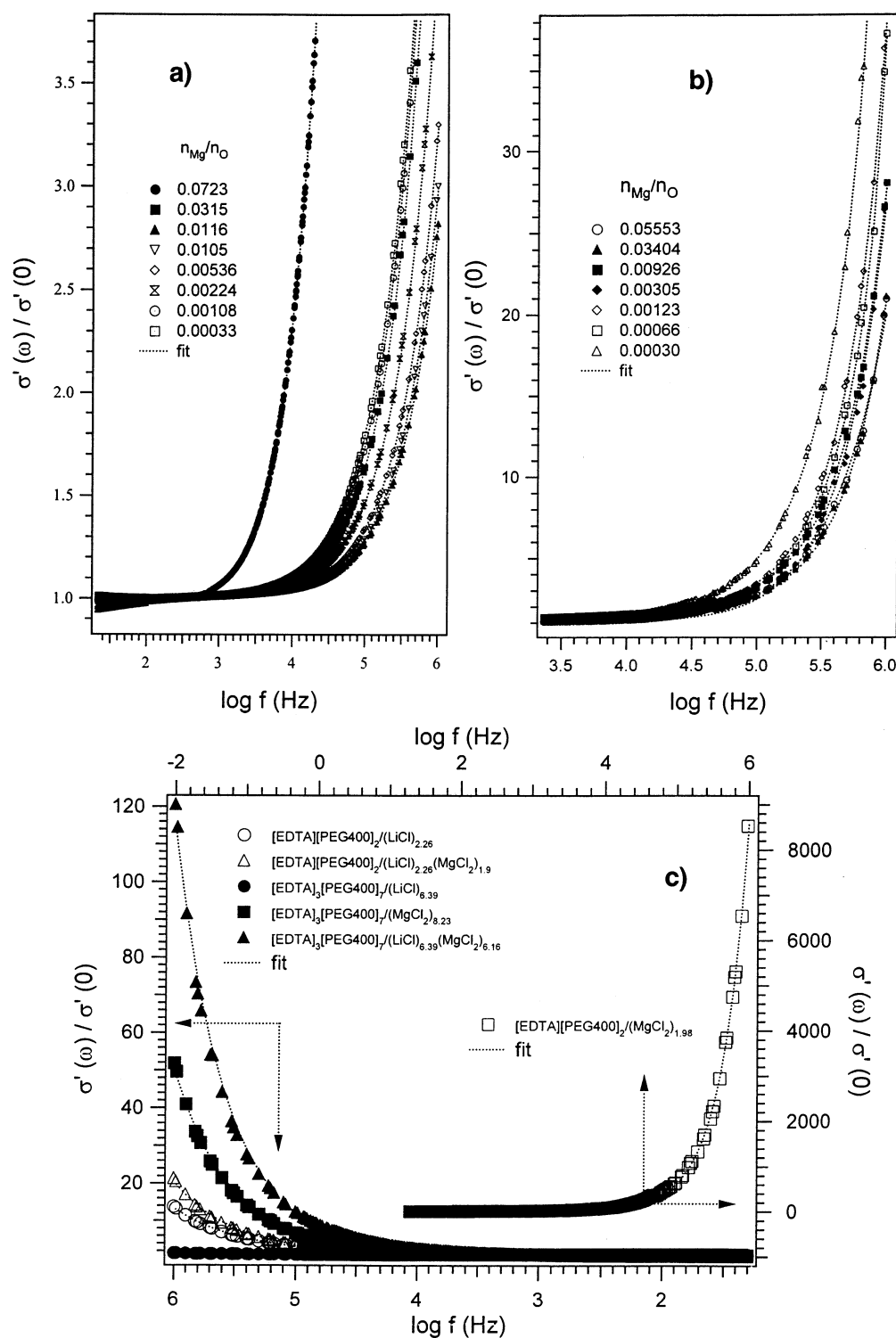


**Figure 8.** Effect of composition on  $\{\sigma'(\omega)/\sigma'(0)\}$  spectra at 20 °C for selected (a) PEG400/(MgCl<sub>2</sub>)<sub>x</sub> and (b) poly[PEG400-alt-DEOS]/(MgCl<sub>2</sub>)<sub>x</sub> complexes; (c) lithium and magnesium electrolytic complexes based on [EDTA][PEG400]<sub>2</sub> and [EDTA]<sub>3</sub>[PEG400]<sub>7</sub> polymers. Simulated curves are shown by dotted lines.

is the thermodynamic ideal glass transition temperature. The dotted curves in Figures 10a and 11 show the results of fitting of eq 2 to the conductivity data by means of nonlinear least-squares methods and assuming a starting  $T_0$  value on the basis of boundary condition  $(T_g - 55) \leq T_0 \leq (T_g - 40)$ ,  $T_g \cong -60$  as suggested in the literature.<sup>34,25,11</sup> It is to be pointed out that the dependence of conductivity on the reciprocal of temperature for PEG400/(MgCl<sub>2</sub>)<sub>x</sub> appears to be very similar to that for the analogous system based on LiCl.<sup>34</sup> Therefore, it is to be expected that the conductivity occurs with a similar ionic migration

mechanism (Figure 10a). On the other hand, in the complexes based on [EDTA][PEG400]<sub>2</sub> and [EDTA]<sub>3</sub>[PEG400]<sub>7</sub> host polymers, the observed VTF profiles demonstrate that the polymer mobility is crucial for conduction. Figure 11, parts a and b, clearly shows that, for both lithium PE materials, an increase in conductivity is observed with respect to pristine polymers, whereas the polymer electrolytes based on MgCl<sub>2</sub> exhibit a decrease in ionic conductivity. In particular, [EDTA][PEG400]<sub>2</sub>/(MgCl<sub>2</sub>)<sub>1.98</sub> exhibits the lowest conductivity, indicating that the chain mobility of the material is strongly reduced

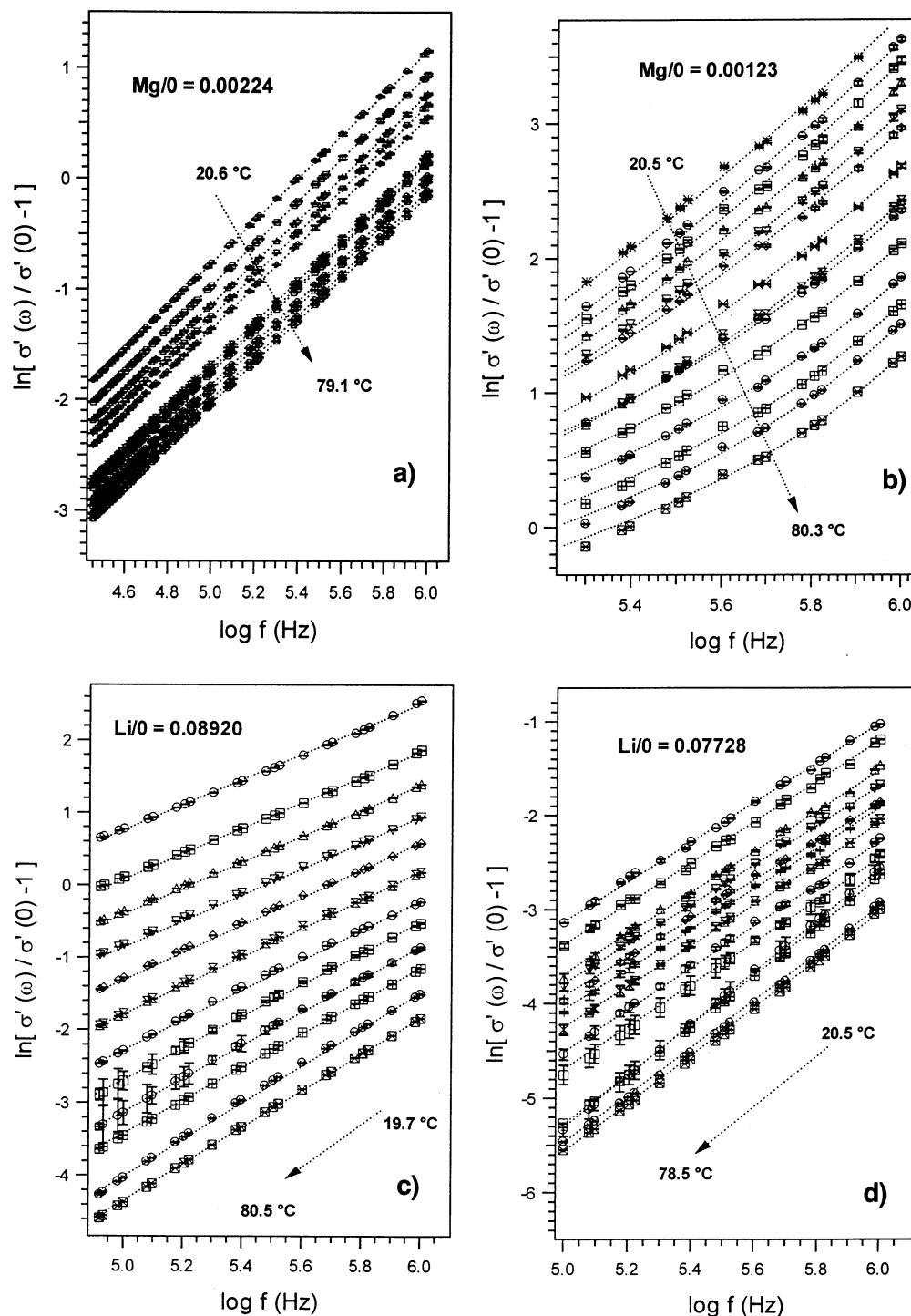


**Figure 9.**  $\ln[\{\sigma'(\omega)/\sigma'(0) - 1\}]$  versus  $\log f$  (Hz) for selected (a) PEG400/(MgCl<sub>2</sub>)<sub>x</sub>; (b) poly[PEG400-*alt*-DEOS]/(MgCl<sub>2</sub>)<sub>x</sub> complexes; lithium electrolytic complexes based on [EDTA][PEG400]<sub>2</sub> (c) and [EDTA]<sub>3</sub>[PEG400]<sub>7</sub> polymers (d). Simulated curves are shown by dotted lines.

because of the presence of Mg-coordination cross-links. The [EDTA]<sub>3</sub>[PEG400]<sub>7</sub>/(LiCl)<sub>6.39</sub>(MgCl<sub>2</sub>)<sub>6.16</sub> polymer electrolyte presents a conductivity curve very similar to that of [EDTA]<sub>3</sub>[PEG400]<sub>7</sub>/(MgCl<sub>2</sub>)<sub>8.23</sub>. Furthermore, the conductivity of the [EDTA][PEG400]<sub>2</sub>/(LiCl)<sub>2.26</sub>(MgCl<sub>2</sub>)<sub>1.9</sub> system is lower than that of the pristine polymer host at temperatures lower than 45 °C and increases and approximates that of [EDTA][PEG400]<sub>2</sub>/(LiCl)<sub>2.26</sub> at  $T > 45$  °C. These observations are in agreement with the results of  $\sigma'(\omega)$  at high frequencies (Figure 8), thus confirming that a single charge-transfer mechanism ( $\alpha$ ) based on cation migration mediated by the segmental motion of polymer host is responsible for ionic conductivity in these materials.

Figure 10b shows that three conductivity regions are present for poly[PEG400-*alt*-DEOS]/(MgCl<sub>2</sub>)<sub>x</sub> complexes and that these thermally activated processes are strongly dependent on salt concentration. These observations are in agreement with the  $\sigma'(\omega)$  results (Figures 3b and 8b) which, as reported above, show the presence of  $\alpha$  and  $\beta$  ionic charge-transfer mechanisms. The contribution of these two types of mechanisms to the overall conductivity depends on temperature and the composition of the poly[PEG400-*alt*-DEOS]/(MgCl<sub>2</sub>)<sub>x</sub> system (Figure 6). Indeed, comparison of Figures 6 and 10b indicates that the  $\beta$  mechanism, associated with the peak at 22 kHz in the  $\sigma'(\omega)$  curves (Figure 3b), contributes less than 10% of the overall conductivity at  $T > 45$  °C. It is interesting to note that the

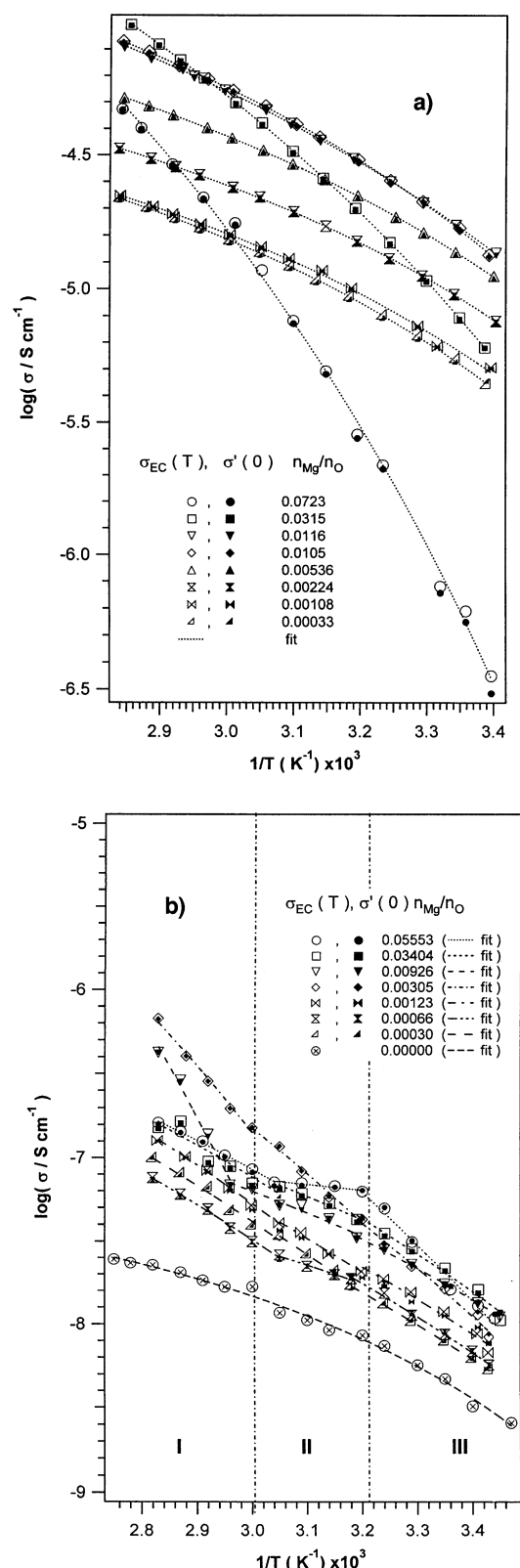


**Figure 10.** Dependence of  $\log \sigma_{EC}(T)$  and  $\log \sigma'(0)$  on temperature. (a) PEG400/(MgCl<sub>2</sub>)<sub>x</sub> complexes; (b) poly[PEG400-*alt*-DEOS]/(MgCl<sub>2</sub>)<sub>x</sub> systems.  $\sigma_{EC}$  is the conductivity determined by equivalent circuit analysis;  $\sigma'(0)$  is the conductivity parameter obtained by fitting eq 1 to  $\sigma'(\omega)$  data. Dotted lines in a and b show VTF and Arrhenius-type fitted curves, respectively.

contribution of this phenomenon depends on the concentration and the salt chemical species present in the bulk material. In particular, the curves of the samples with Mg/O = 0.00305,

0.00926, and 0.03404 greatly in Figure 10b differ from the other profiles, and the same information is revealed in Figure 6.

Further information on the conductivity mechanism in the PEs was obtained by studying the relaxation times  $\tau_{peak}$  and  $\tau_1$  determined from the maxima of the Debye peaks and by fitting eq 1 to the  $\sigma'(\omega)$  data (Figures 3 and 4, respectively). In agreement with ref 34, the temperature dependences of  $\tau_{peak}$  (the conductivity relaxation time) and  $\tau_1$  (a time correlated to the initial site relaxation time  $\tau_2$ , see eq 1) are of the Arrhenius type (data not shown):

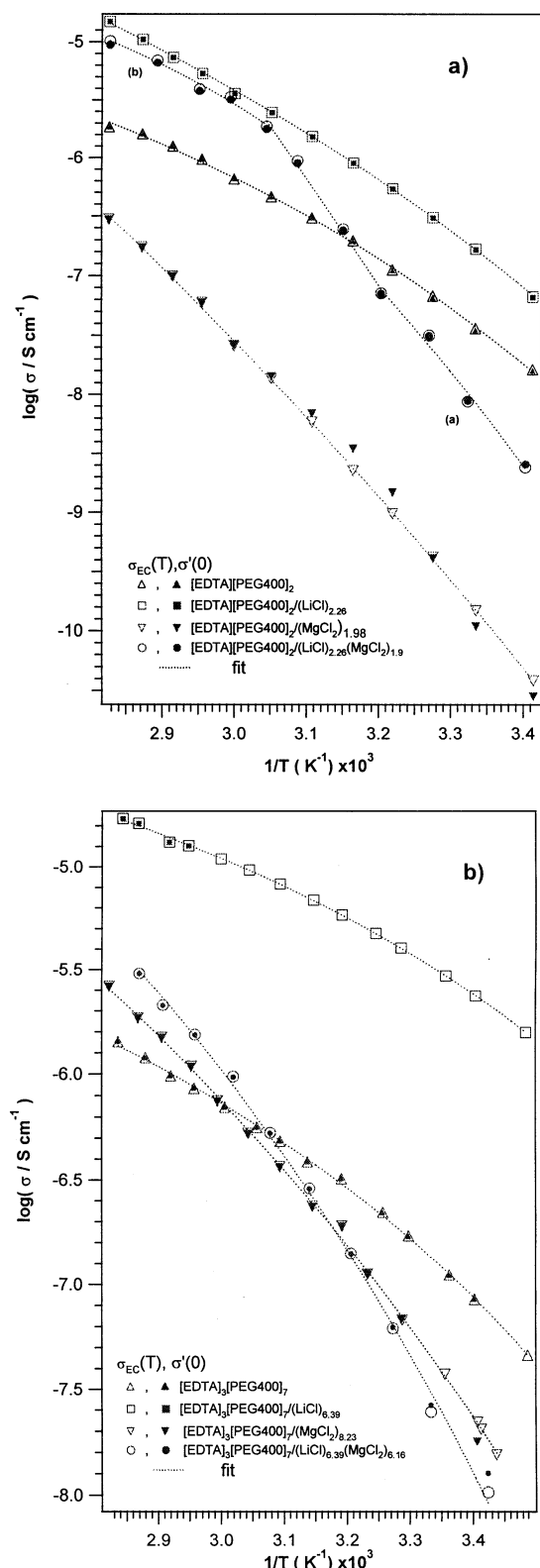
$$\tau_{peak} = \tau_{0,peak} e^{E_{peak}/RT} \quad (3)$$

$$\tau_1 = \tau_{0,1} e^{E_1/RT} \quad (4)$$

where  $\tau_{0,peak}$  and  $\tau_{0,1}$  are preexponential constants,  $E_{peak}$  is the activation energy for the thermally stimulated conductivity relaxation time and  $E_1$  is the site relaxation energy barrier height. The following should be highlighted: (a)  $\ln \tau_{peak}$  and  $\ln \tau_1$  show a similar dependence on the reciprocal of temperature and salt concentration in PEG400/(MgCl<sub>2</sub>)<sub>x</sub>. (b) For poly[PEG400-*alt*-DEOS]/(MgCl<sub>2</sub>)<sub>x</sub> complexes, a plot of  $\ln \tau_{peak}$  against the reciprocal of temperature reveals the same salt concentration effect and the same three conductivity regions detected in Figure 10b. Moreover, plots of the logarithms of  $\tau_{1,\alpha}$  and  $\tau_{1,\beta}$  (obtained with eq 1 for  $N = 2$  and assigned to the two relaxation events  $\alpha$  and  $\beta$ ) against  $1/T$  exhibit Arrhenius type behaviors. (c)  $\ln \tau_{peak}$  and  $\ln \tau_1$  for systems based on [EDTA]<sub>3</sub>[PEG400]<sub>7</sub> present a single linear behavior for each complex that is well described by eqs 3 and 4, respectively.

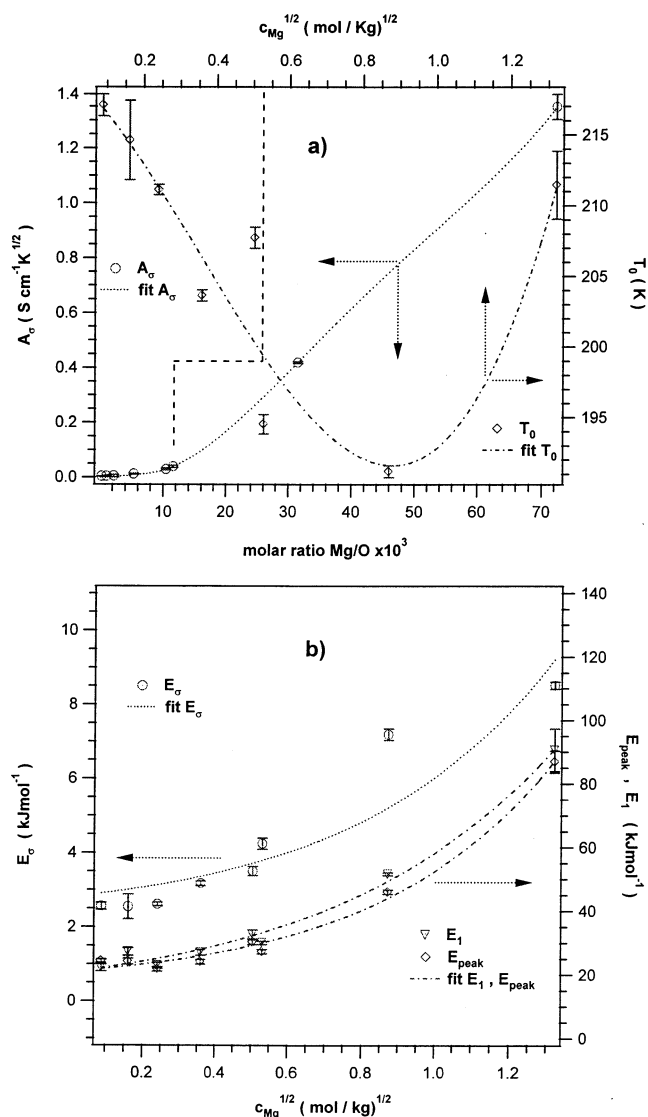
Figure 12, parts a and b report the dependence of  $A_\sigma$ ,  $T_0$ , and  $E_\sigma$  on concentration, i.e.,  $c_{Mg}^{1/2}$  (mol/kg)<sup>1/2</sup>, for PEG400/(MgCl<sub>2</sub>)<sub>x</sub> complexes.  $A_\sigma$  and  $E_\sigma$  increase monotonically, and  $T_0$  exhibits a minimum at  $c_{Mg}^{1/2} \approx 0.85$  (mol/kg)<sup>1/2</sup>. These findings are in agreement with the literature<sup>34</sup> and with results of vibrational studies<sup>39</sup> and indicate that cationic magnesium species (Mg<sup>2+</sup> and [MgCl]<sup>+</sup>) are accommodated in the coordination sites provided by the ether oxygen atoms present along the TGT chains of PEG400. However, as the salt concentration increases, the concentration of Cl<sup>-</sup> ions not interacting with the hydrogen atoms of terminal PEG400 hydroxyls also rises, thus increasing the concentration of [Mg-Cl]<sup>+</sup> species distributed along the PEG chains. At  $c_{Mg}^{1/2} > 0.5$  (mol/kg)<sup>1/2</sup>, these species reduce  $T_0$ , raise the fitting parameter  $E_\sigma$ , and markedly increase  $A_\sigma$ .

Table 2a reports the values of  $E_\sigma$ ,  $E_{peak}$ ,  $E_{1,\alpha}$ , and  $E_{1,\beta}$  on  $c_{Mg}^{1/2}$  for poly[PEG400-*alt*-DEOS]/(MgCl<sub>2</sub>)<sub>x</sub> complexes in the regions I, II, and III.  $E_\sigma$  and  $E_{peak}$  have been determined by fitting  $y = A_\sigma e^{-E_i/R(T-T_0)}$  (with  $i = \sigma, peak$ ) to the conductivity data reported in Figure 10b and to  $\ln \tau_{peak}$  (data not shown). In agreement with the literature,<sup>51,52,34</sup> in fitting procedures, the starting value of  $T_0$  was assumed -162 K.  $E_{1,\alpha}$  and  $E_{1,\beta}$  have been determined by fitting eq 4 to the two relaxation times associated with the hopping mechanisms  $\alpha$  and  $\beta$ .  $E_{1,\alpha}$  and  $E_{1,\beta}$  indicate three possible compositional regions. In region (i) at  $c_{Mg}^{1/2} < 0.22$  (mol/kg)<sup>1/2</sup>, it can be observed that the activation energy of process  $\alpha$  is lower than that of  $\beta$ . In region  $0.22 \leq c_{Mg}^{1/2} \leq 0.84$  (mol/kg)<sup>1/2</sup>, processes  $\alpha$  and  $\beta$  both occur with quite the same activation energies. This reflects the fact that at high temperatures the activation energies are quite similar, whereas  $E_{peak,III}$  and  $E_{\sigma,III}$  present the highest values. Finally, in region (iii) at  $c_{Mg}^{1/2} > 0.84$  (mol/kg)<sup>1/2</sup>, the charge migration is again dominated by process  $\alpha$ , and the activation energies determined from Debye peaks and conductivity data are similar. Table 2b



**Figure 11.** Dependence of  $\log \sigma_{EC}(T)$  and  $\log \sigma'(0)$  on temperature for lithium and magnesium electrolytic complexes based on [EDTA]-[PEG400]<sub>2</sub> (a) and [EDTA]<sub>3</sub>[PEG400]<sub>7</sub> polymers (b).  $\sigma_{EC}$  is the conductivity determined by equivalent circuit analysis;  $\sigma'(0)$  is the conductivity parameter obtained by fitting eq 1 to  $\sigma'(\omega)$  data. Dotted lines show VTF fitted curves.

summarize the activation energies determined through eqs 2–4 using the measurements determined for the PE samples based on [EDTA][PEG400]<sub>2</sub> and [EDTA]<sub>3</sub>[PEG400]<sub>7</sub> host polymers. It is to be observed that the  $E_{\sigma}$  values determined for magnesium



**Figure 12.**  $A_{\sigma}$  and  $T_0$  (a) and  $E_{\sigma}$ ,  $E_{peak}$ , and  $E_1$  (b) as a function of salt concentration for PEG400/(MgCl<sub>2</sub>)<sub>x</sub>.

ion derivatives present the highest values, whereas those of lithium based materials are the lowest. The presence of lithium ions in the mixed salt polymer electrolytes limits the increase in activation energies. These results are further supported by the  $T_0$  values which demonstrate that  $T_0$  decreases in the order Li + Mg ≤ Li < Mg for both polymer electrolytes. It can therefore be concluded that the overall conductivity is highly dependent on the salt concentration in the polymer host and on the types of coordination sites present in the host materials. Further information regarding the conductivity mechanism in the investigated systems is provided by analyzing the temperature dependence of the parameter  $p = (\text{initial back-hop rate}) / (\text{initial site relaxation rate})$ . Indeed, the conductivity due to ion hopping is successful<sup>45</sup> when the initial site relaxation rate,  $r_s = 1/\tau_s$ , is higher than the initial back-hop rate,  $r_b = 1/\tau^*$ , of the ionic species. Figure 13a–d shows the dependence of the  $p$  values of the investigated systems on temperature. In particular,  $p < 1$  is always observed for PEG400/(MgCl<sub>2</sub>)<sub>x</sub> complexes (Figure 13a). For poly[PEG400-*alt*-DEOS]/(MgCl<sub>2</sub>)<sub>x</sub> compounds, this condition is satisfied only for hopping process  $\alpha$  (Figure 13b), whereas for  $\beta$  process,  $p > 1$  was observed for all of the samples (Figure 13c). This second result indicates that the back-hop rate is always higher than the initial site relaxation rate. This phenomenon is likely to be possible if the



**TABLE 2: Activation Energies as a Function of Salt Concentration in Poly[PEG400-*alt*-DEOS]/(MgCl<sub>2</sub>)<sub>x</sub> Systems (a) and in Lithium and Magnesium Electrolytic Complexes Based on [EDTA][PEG400]<sub>2</sub> and [EDTA]<sub>3</sub>[PEG400]<sub>7</sub> Polymers (b)<sup>a</sup>**

(a) Complex Poly[PEG400- <i>alt</i> -DEOS]/(MgCl <sub>2</sub> ) <sub>x</sub>									
$c_{\text{Mg}}^{1/2\ b}$ (mol/kg) <sup>1/2</sup>	$E_{\sigma, \text{I}}^e$ (kJ mol <sup>-1</sup> )	$E_{\sigma, \text{II}}^c$ (kJ mol <sup>-1</sup> )	$E_{\sigma, \text{III}}^c$ (kJ mol <sup>-1</sup> )	$E_{\text{peak, I}}^c$ (kJ mol <sup>-1</sup> )	$E_{\text{peak, II}}^c$ (kJ mol <sup>-1</sup> )	$E_{\text{peak, III}}^c$ (kJ mol <sup>-1</sup> )	$E_{1, \alpha}^d$ (kJ mol <sup>-1</sup> )	$E_{1, \beta}^d$ (kJ mol <sup>-1</sup> )	compositional regions
1.088	13.5 ± 0.5	1.59 ± 0.05	9.12 ± 0.06	13.3 ± 0.7	0.25 ± 0.09	9.7 ± 0.2	1.81 ± 0.02	5.94 ± 0.09	}(iii)
0.852	9.1 ± 0.4	6.47 ± 0.09	10.05 ± 0.5	8.9 ± 0.5	6.2 ± 0.1	10.1 ± 0.7	2.34 ± 0.01	3.84 ± 0.03	
0.444	7.58 ± 0.03	6.4 ± 0.3	32.9 ± 0.6	7.0 ± 0.1	6.2 ± 0.5	33.2 ± 0.3	4.32 ± 0.03	3.27 ± 0.04	
0.255	11.6 ± 0.3	13.5 ± 0.2	20.3 ± 0.3	11.5 ± 0.5	13.4 ± 0.3	20.4 ± 0.5	4.46 ± 0.1	4.20 ± 0.08	}(ii)
0.163	8.3 ± 0.3	9.4 ± 0.1	12.05 ± 0.06	9.6 ± 0.4	9.8 ± 0.4	9.7 ± 0.4	2.30 ± 0.05	5.48 ± 0.07	
0.118	8.57 ± 0.09	5.20 ± 0.05	10.8 ± 0.1	8.35 ± 0.05	5.5 ± 0.3	11.4 ± 0.1	1.85 ± 0.02	5.5 ± 0.1	}(i)
0.080	8.30 ± 0.01	10.71 ± 0.06	11.2 ± 0.3	9.7 ± 0.1	9.7 ± 0.1	9.7 ± 0.1	3.20 ± 0.07	5.61 ± 0.02	
(b)									
complex	$E_{\sigma}$ (kJ mol <sup>-1</sup> )	$E_{\text{peak}}$ (kJ mol <sup>-1</sup> )	$E_1$ (kJ mol <sup>-1</sup> )						
[EDTA][PEG400] <sub>2</sub> /(LiCl) <sub>2.26</sub>	15.4 ± 0.2	75.6 ± 1.6	69.1 ± 0.9						
[EDTA][PEG400] <sub>2</sub> /(MgCl <sub>2</sub> ) <sub>1.98</sub>	29.8 ± 0.6	119.1 ± 1.0	91.6 ± 0.8						
[EDTA][PEG400] <sub>2</sub> /(LiCl) <sub>2.26</sub> (MgCl <sub>2</sub> ) <sub>1.9</sub>	6.51 ± 0.08 (a) <sup>e</sup>	124.5 ± 1.5	76.0 ± 1.1						
	3.94 ± 0.07 (b)								
[EDTA] <sub>3</sub> [PEG400] <sub>7</sub> /(LiCl) <sub>6.39</sub>	4.05 ± 0.03	29.0 ± 0.6	21.27 ± 0.09						
[EDTA] <sub>3</sub> [PEG400] <sub>7</sub> /(MgCl <sub>2</sub> ) <sub>8.23</sub>	13.3 ± 0.1	70.5 ± 0.8	62.6 ± 0.7						
[EDTA] <sub>3</sub> [PEG400] <sub>7</sub> /(LiCl) <sub>6.39</sub> (MgCl <sub>2</sub> ) <sub>6.16</sub>	12.6 ± 0.5	85.5 ± 1.2	74.4 ± 1.3						

<sup>a</sup>  $E_{\sigma}$ ,  $E_{\text{peak}}$ , and  $E_1$  are the activation energies determined respectively from conductivity data, conductivity relaxation times and initial site relaxation times. <sup>b</sup>  $c = \text{mol}_{\text{MgCl}_2}/\text{kg}_{\text{polymer}}$ . <sup>c</sup> The indices I, II, and III correspond to the three conductivity regions shown in Figure 10b. <sup>d</sup> The indices  $\alpha$  and  $\beta$  indicate the relaxation events detected by fitting eq 1 for  $N = 2$  to the data of Figure 3b. <sup>e</sup> (a) and (b) correspond to the conductivity regions shown in Figure 11a.

ionic migration takes place through an anionic hopping mechanism. Indeed, in this case, after an anion hop between magnesium species coordinated by polyether oxygen atoms, it is expected that geometrical arrangement of sites would be negligible. Therefore, a decrease in the site relaxation rate is expected. Figure 13d shows that the  $p$  values for the polymer electrolytes based on [EDTA][PEG400]<sub>2</sub> and [EDTA]<sub>3</sub>[PEG400]<sub>7</sub> host are always much less than unity. Particularly, it is to be noted that (a) for both [EDTA][PEG400]<sub>2</sub>/(LiCl)<sub>2.26</sub> and [EDTA]<sub>3</sub>[PEG400]<sub>7</sub>/(LiCl)<sub>6.39</sub>  $p$  rises as the temperature increases and (b) for magnesium containing polymer electrolytes the opposite behavior is observed. These results seem to indicate that the increase in temperature enhances the site relaxation rate, which becomes higher in magnesium containing polymers compared to polymer electrolytes based on lithium salts. It is likely that as the temperature increases lithium ions are less coordinated in the polymer sites owing to the thermal energy. These indications suggest that ion hopping with consequent site relaxation contributes significantly to the overall conductivity of the investigated PE materials and that this contribution is mainly regulated by the segmental motion of the host chains.

**3.3. Equivalent Conductivity Studies.** To detect possible ion association interactions in the PEG400/(MgCl<sub>2</sub>)<sub>x</sub> and poly[PEG400-*alt*-DEOS]/(MgCl<sub>2</sub>)<sub>x</sub> complexes, the equivalent conductivity ( $\Lambda$ ) was analyzed with respect to the magnesium chloride concentration,  $c_{\text{Mg}}^{1/2}$  (mol/kg)<sup>1/2</sup>. The resulting isothermal  $c_{\text{Mg}}^{1/2}$  curves for the PEG400/(MgCl<sub>2</sub>)<sub>x</sub> and poly[PEG400-*alt*-DEOS]/(MgCl<sub>2</sub>)<sub>x</sub> systems are shown in Figures 14a and 15a, respectively. It should be observed that for the PEG400/(MgCl<sub>2</sub>)<sub>x</sub> system (Figure 14a), an exponential decrease in equivalent conductivity is observed as  $c_{\text{Mg}}^{1/2}$  increases; in agreement with ref 34, these profiles are reproduced by applying the equation

$$\Lambda = H_0 + K_1 e^{-\alpha_1 c_{\text{Mg}}^{1/2}} + K_2 e^{-\alpha_2 c_{\text{Mg}}^{1/2}} \quad (5)$$

where  $H_0$ ,  $K_i$ , and  $\alpha_i$  ( $i = 1$  and  $2$ ) are fitting parameters (see dotted curves in Figure 14a). These  $\Lambda$  profiles show the typical decrease already observed for other polymer electrolyte materi-

als.<sup>1,34,53</sup> This decrease in  $\Lambda$  can be attributed to strong cation–anion interactions,<sup>1,34,54</sup> which reduce the charge of Mg<sup>2+</sup> cations giving rise to conducting cation species [Mg–Cl]<sup>+</sup> with subsequent formation of electrically neutral ion pairs of the type [MgCl]<sup>+</sup>···Cl<sup>-</sup>. For  $c_{\text{Mg}}^{1/2} \ll 1$  (mol/kg)<sup>1/2</sup>, eq 5 approximates an Onsager type relation<sup>54</sup>

$$\Lambda = \Lambda_0 - A c_{\text{Mg}}^{1/2} \quad (6)$$

where  $\Lambda_0 = H_0 + K_1 + K_2$  and  $A = K_1 \alpha_1 + K_2 \alpha_2$ .

It is observed that  $\Lambda_0$  and  $A$ , which correspond to the parameters of the equivalent conductivity at infinite dilution,<sup>34</sup> exhibit typical VTF behavior, thus indicating that they are correlated with chain mobility (see Figure 14b).

The equivalent conductivities of the poly[PEG400-*alt*-DEOS]/(MgCl<sub>2</sub>)<sub>x</sub> system (Figure 15a) exhibit the typical profiles observed for other PE systems.<sup>1</sup> In accordance with these previous studies and the results presented above, the steep decrease in the equivalent conductivity at  $c_{\text{Mg}}^{1/2} \leq 0.14$  (mol/kg)<sup>1/2</sup> can be attributed to the strong cation–anion interactions. Between 0.14 and 0.22 (mol/kg)<sup>1/2</sup>, the molar conductivity rises. In agreement with previous impedance results and Raman scattering measurements on PPO–LiCF<sub>3</sub>SO<sub>3</sub> complexes,<sup>1,55</sup> one can propose that this phenomenon occurs because the ionic mobility is enhanced in this concentration region owing to the anion migration between magnesium cationic species. A decline in  $\Lambda$  is observed at  $c_{\text{Mg}}^{1/2} \geq 0.22$  (mol/kg)<sup>1/2</sup> because of the increase in neutral magnesium salt species which in turn reduces the effect of mobility enhancement caused by anion migration. The equivalent conductivity data at  $c_{\text{Mg}}^{1/2} \ll 1$  (mol/kg)<sup>1/2</sup> exhibit the same Onsager type eq 6. The parameters of this equation show the same typical dependence of VTF on temperature (Figure 15b), thus indicating that, also in this case, segmental motion is a crucial factor in determining conductivity, independent of the presence or absence of ion–ion interactions.

#### 4. Conclusions

This report describes electrical spectroscopy investigations performed on four polymer electrolytes in the 20 Hz to 1 MHz

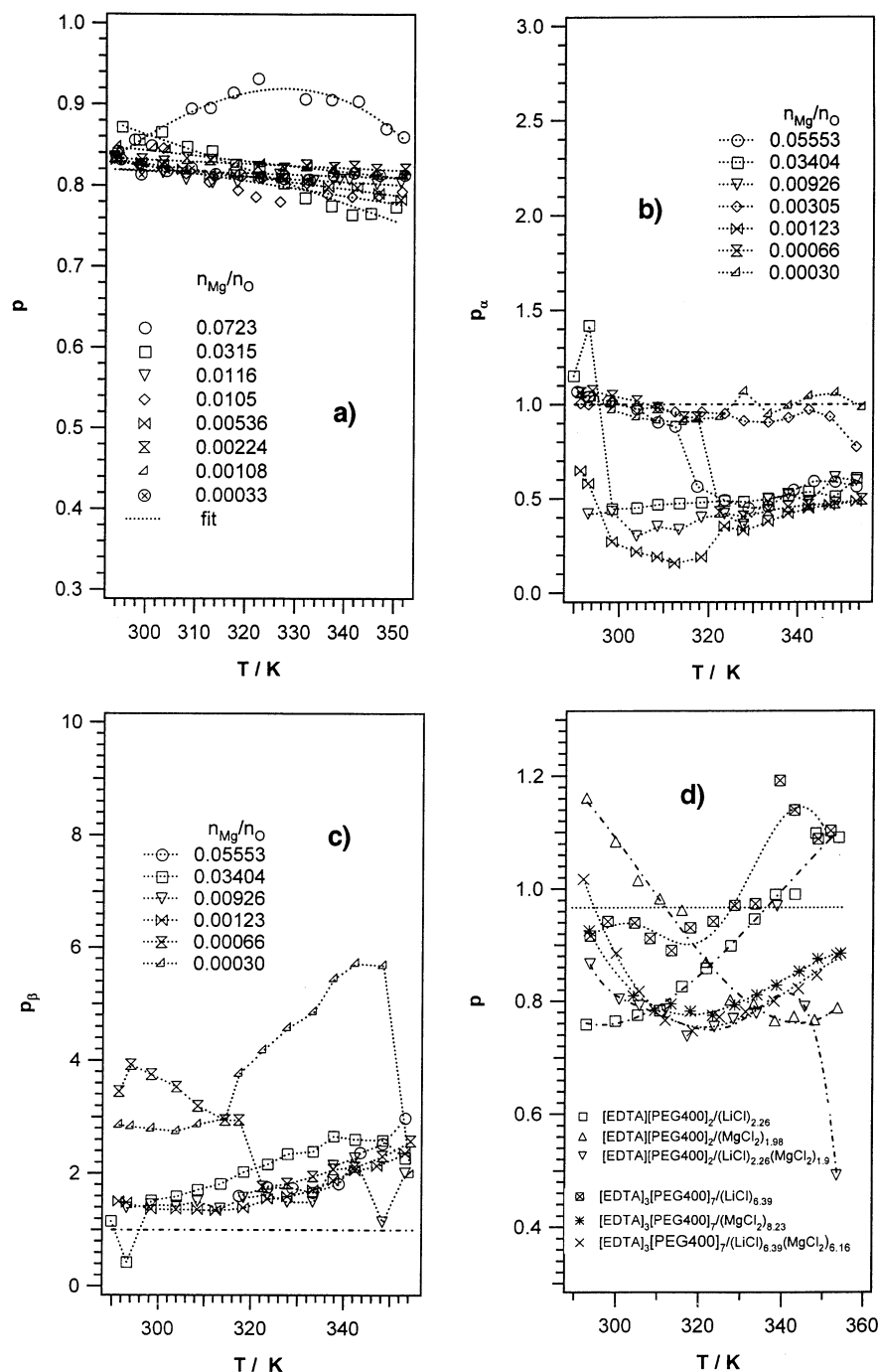


**Figure 13.** Plot of  $p$  as a function of temperature. (a) PEG400/(MgCl<sub>2</sub>)<sub>x</sub> complexes; (b) process  $\alpha$  in poly[PEG400-alt-DEOS]/(MgCl<sub>2</sub>)<sub>x</sub> systems; (c) process  $\beta$  in poly[PEG400-alt-DEOS]/(MgCl<sub>2</sub>)<sub>x</sub> systems; (d) lithium and magnesium electrolytic complexes based on [EDTA][PEG400]<sub>2</sub> and [EDTA]<sub>3</sub>[PEG400]<sub>7</sub> polymers.

range and at temperatures ranging from 20 to 80 °C. In particular, real and imaginary components of the impedance of PEG400/(MgCl<sub>2</sub>)<sub>x</sub> ( $0.00329 \leq x \leq 0.7000$ ); poly[PEG400-alt-DEOS]/(MgCl<sub>2</sub>)<sub>x</sub> ( $6.28 \times 10^{-2} \leq x \leq 13.16$ ); [EDTA][PEG400]<sub>2</sub>/(LiCl)<sub>2.26</sub>; [EDTA][PEG400]<sub>2</sub>/(MgCl<sub>2</sub>)<sub>1.98</sub>; [EDTA][PEG400]<sub>2</sub>/(LiCl)<sub>2.26</sub>(MgCl<sub>2</sub>)<sub>1.9</sub>; [EDTA]<sub>3</sub>[PEG400]<sub>7</sub>/(LiCl)<sub>6.39</sub>; [EDTA]<sub>3</sub>[PEG400]<sub>7</sub>/(MgCl<sub>2</sub>)<sub>8.23</sub>; and [EDTA]<sub>3</sub>[PEG400]<sub>7</sub>/(LiCl)<sub>6.39</sub>(MgCl<sub>2</sub>)<sub>6.16</sub> were studied. Full characterization of the AC electrical response of these PEs was carried out by equivalent circuit and correlated ionic motion analysis performed by using a generalized UPL equation. Comparison of the bulk conductivity data determined by using both these methods indicated their perfect equivalence for studying the electrical response of these materials in the medium-frequency range.

However, it was demonstrated that application of the G-UPL method to analyze the  $\sigma'(\omega)$  spectrum at frequencies higher than 1 kHz provides the exact bulk conductivity of the materials without any equivalent circuit assumptions for the cell. Moreover, the investigations carried out in the PEG400/(MgCl<sub>2</sub>)<sub>x</sub> and poly[PEG400-alt DEOS]/(MgCl<sub>2</sub>)<sub>x</sub> systems allowed us to establish that the ionic species formed in the bulk materials are crucial for the overall conductivity as well as for the well-known "segmental motion". Indeed, results suggest that the conductivity in PEG400/(MgCl<sub>2</sub>)<sub>x</sub> complexes takes place through hopping of the Mg<sup>2+</sup> and [MgCl]<sup>+</sup> cation species ( $\alpha$  event) between the sites present in the material along the polyether chains (intra-CH hopping or inter-CH hopping). This latter hopping event results in conduction if it is followed by correlation motions

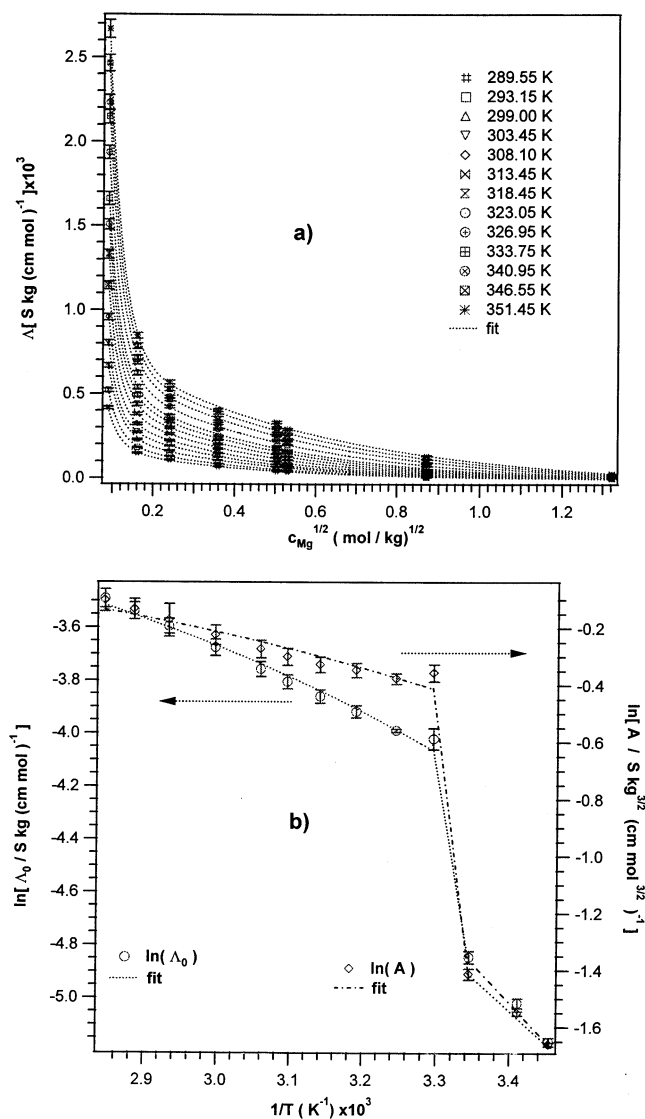


**Figure 14.** PEG400/(MgCl<sub>2</sub>)<sub>x</sub> complexes. (a) Equivalent conductivity as a function of salt concentration; (b)  $\Lambda_0$  and  $A$  parameters of Onsager type eq 6 versus the reciprocal of temperature.

and geometrical relaxation<sup>34</sup> of sites. These indications were confirmed by the equivalent conductivity analysis, which showed an increase in strong cation–anion interactions in the bulk material as the salt concentration increases. It is reasonable to conclude that in PEG400/(MgCl<sub>2</sub>)<sub>x</sub> complexes the conductivity at low salt concentrations is due to Mg<sup>2+</sup> cation migration, whereas at high salt concentration, the cationic [MgCl]<sup>+</sup> species contribute significantly to the overall conductivity.

The studies carried out on poly[PEG400-*alt*-DEOS]/(MgCl<sub>2</sub>)<sub>x</sub> polymer electrolytes clarified the importance of the concentration of hydroxyl groups in the determination of the cation species. Indeed, because of the low concentration of anions involved in the hydrogen bonding cage,<sup>25</sup> the concentration of magnesium species, e.g., [MgCl]<sup>+</sup> and [MgCl]<sup>+</sup>...Cl<sup>-</sup>, bonded to the polyether moieties of the polymer is high. Coordination of these species to the polyether chains is responsible for two types of migration mechanisms. The first mechanism,  $\alpha$ , is ascribed to the migration of cationic Mg<sup>2+</sup> and [MgCl]<sup>+</sup> species. This process is similar to that detected for PEG400/(MgCl<sub>2</sub>)<sub>x</sub> complexes and occurs via a hopping mechanism followed by host medium reorganization. These hypotheses are supported by the value of the  $p$  parameter derived from eq 1, which was found to be less than unity.

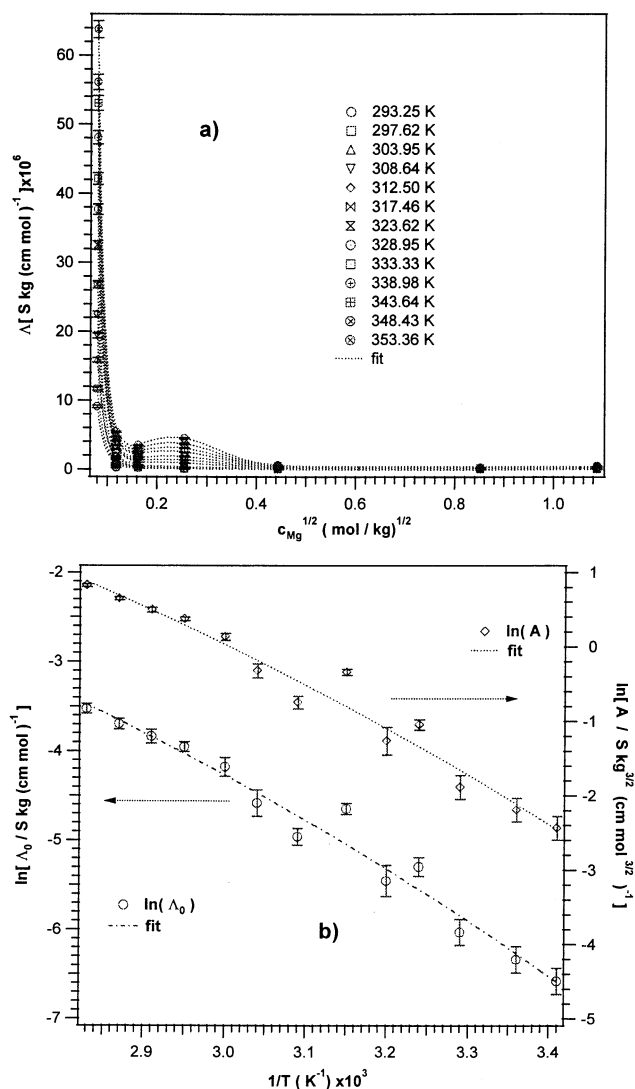


**Figure 15.** Poly[PEG400-*alt*-DEOS]/(MgCl<sub>2</sub>)<sub>x</sub> electrolytic complexes. (a) Equivalent conductivity as a function of salt concentration; (b)  $\Lambda_0$  and  $A$  parameters of Onsager type eq 6 versus the reciprocal of temperature.

On the other hand, analysis of the  $\sigma'(\omega)$  profiles revealed an additional charge migration mechanism at 22 kHz ( $\beta$  event). It should be pointed out that the presence of two concurrent conductivity mechanisms in poly[PEG400-*alt*-DEOS]/(MgCl<sub>2</sub>)<sub>x</sub> host materials is also indicated by the plots of  $\log \sigma$  versus  $1/T$ . Indeed, three conductivity regions are detected in these latter profiles.

The analysis of  $\sigma'(\omega)$  in terms of the UPL equation revealed that  $p$  is greater than 1 for the  $\beta$  mechanism. This observation leads to the hypothesis that the back-hop process occurs at a higher rate with respect to the site relaxation phenomenon. This suggests that  $\beta$  mechanism could be associated with hopping of Cl<sup>-</sup> between magnesium species coordinated by the oxygen donor atoms of polyether chains. As a result, in this case, cation migration is observed without any substantial geometric site relaxation. It is clear that this latter process increases the ionic mobility of the cation. This was confirmed by the increase in equivalent conductivity in the  $0.18 \leq c_{Mg}^{1/2} \leq 0.44$  (mol/kg)<sup>1/2</sup> region and by the decrease in the activation energy associated with  $\beta$  migration mechanism in this region. At  $c_{Mg}^{1/2} \geq 0.44$  (mol/kg)<sup>1/2</sup>, the solvent separated [MgCl]<sup>+</sup> species are transformed into dynamic PEG–MgCl<sub>2</sub>Mg–PEG cross-links. The presence of these cross-links increases the viscosity of the

material and decreases its equivalent conductivity. The studies carried out on polymer electrolytes based on [EDTA][PEG400]<sub>2</sub> and [EDTA]<sub>3</sub>[PEG400]<sub>7</sub> demonstrated that the EDTA coordination site is selective toward magnesium ion species. This strong coordination inhibits the conductivity of these systems in two different ways: first by reducing the concentration of magnesium cation species able to migrate and second by decreasing the segmental mobility of host materials owing to the formation of magnesium-ion coordination cross-links between different host polymer chains. Electrical spectroscopy measurements revealed that lithium ions are the most mobile cations in these systems and that this ion preferentially interacts with both of the oxygen atoms of the EDTA sites and polyether moieties. As demonstrated by the *p* values of less than unity, the ionic conductivity in EDTA based polymer electrolytes takes place with a mechanism similar to that described above for the PEG400/(MgCl<sub>2</sub>)<sub>x</sub> and PEG400/(LiCl)<sub>x</sub><sup>34</sup> complexes (α). These indications are supported by the activation energies. Taken together, the results of impedance spectroscopy carried out on [EDTA][PEG400]<sub>2</sub> and [EDTA]<sub>3</sub>[PEG400]<sub>7</sub> complexes indicated that the type and geometry of coordination sites present in the polymer host are of crucial importance in the modulation of the conductivity of polymer electrolytes. In particular, sites which are able to strongly coordinate cations seem to be excluded from the overall conductivity mechanism.

In conclusion, the overall conductivity of the investigated polymer electrolytes is regulated by migrating ionic species present in the bulk material, by the type of coordination sites in the host polymer, and by the types of macromolecular mobilities.

## References and Notes

- (1) Gray, F. M. *Polymer Electrolytes*, RSC Materials Monographs; Royal Society of Chemistry: Cambridge, U.K., 1997.
- (2) Scrosati, B.; Neat, R. J. In *Applications of Electroactive Polymers*; Scrosati, B., Ed.; Chapman and Hall: London, 1993; p 182.
- (3) Wright, P. W. *Electrochim. Acta* **1998**, *43*, 1137.
- (4) Dias, F. B.; Plomb, L.; Veldhuis, J. B. *J. Power Sources* **2000**, *88*, 169.
- (5) Di Noto, V. *J. Mater. Res.* **1997**, *12*, 3393.
- (6) Di Noto, V.; Furlani, M.; Lavina, S. *Polym. Adv. Technol.* **1996**, *7*, 759.
- (7) Münchow, V.; Di Noto, V.; Tondello, E. *Electrochim. Acta* **2000**, *45*, 1211.
- (8) Di Noto, V. *J. Phys. Chem. B* **2000**, *104*, 10116.
- (9) Di Noto, V.; Fauri, M.; Vittadello, M.; Lavina, S.; Biscazzo, S. *Electrochim. Acta* **2001**, *46*, 1586.
- (10) Ratner, M.; Shriver, D. F. *Chem. Rev.* **1988**, *88*, 109.
- (11) Ratner, M. In *Polymer Electrolyte Reviews-I*; McCallum, J. R., Vincent, C. A., Eds; Elsevier Applied Science: New York, 1989; Chapter 7.
- (12) Ratner, M.; Nitzan, A. *Faraday Discuss. Chem. Soc.* **1989**, *88*, 19.
- (13) Neyertz, S.; Brown, D.; Thomas, J. O. *J. Chem. Phys.* **1994**, *101*, 10064.
- (14) Neyertz, S.; Brown, D.; Thomas, J. O. *Electrochim. Acta* **1995**, *40*, 2063.
- (15) Neyertz, S.; Brown, D. *J. Chem. Phys.* **1995**, *102*, 9275.
- (16) Lin, B.; Boinske, P. T.; Halley, J. W. *J. Chem. Phys.* **1996**, *105*, 1668.
- (17) Smith, G. D.; Yoon, D. Y.; Jaffe, R. L.; Colby, R. H.; Krishnamoorti, R.; Fetters, L. J. *Macromolecules* **1996**, *29*, 3462.
- (18) Hyun, J. K.; Dong, H.; Rodas, C. P.; Frech, R.; Wheeler, R. A. *J. Phys. Chem. B* **2001**, *105*, 3329.
- (19) Druger, S. D.; Nitzan, A.; Ratner, M. A. *J. Chem. Phys.* **1983**, *79*, 3133.
- (20) Druger, S. D.; Ratner, M. A.; Nitzan, A. *Phys. Rev. B* **1985**, *31*, 3939.
- (21) Furukawa, T.; Imura, M.; Yuruzume, H. *Jpn. J. Appl. Phys.* **1997**, *36*, 1119.
- (22) Furukawa, T.; Yoneya, K.; Takahashi, Y.; Ito, K.; Ohno, H. *Electrochim. Acta* **2000**, *45*, 1443.
- (23) Di Noto, V.; Bettinelli, M.; Furlani, M.; Lavina, S.; Vidali, M. *Macromol. Chem. Phys.* **1996**, *197*, 375.
- (24) Albinson, I.; Mellander, B. E.; Stevens, J. R. *J. Chem. Phys.* **1992**, *96*, 681.
- (25) Di Noto, V.; Longo, D.; Münchow, V. *J. Phys. Chem. B* **1999**, *103*, 2636.
- (26) Nuttall, R. H.; Stalker, D. M. *Talanta* **1977**, *24*, 355.
- (27) Gillis, J. N.; Sievers, R. E. *Anal. Chem.* **1985**, *57*, 1572.
- (28) Di Noto, V.; Bresadola, S. *Macromol. Chem. Phys.* **1996**, *197*, 3827.
- (29) Loneragan, M. C.; Perram, J. W.; Ratner, M.; Shriver, D. F. *J. Chem. Phys.* **1993**, *98*, 4937.
- (30) Loneragan, M. C.; Nitzan, A.; Ratner, M.; Shriver, D. F. *J. Chem. Phys.* **1995**, *103*, 3253.
- (31) Roling, B.; Martiny, C.; Funke, K. *J. Non-Cryst. Solids* **1999**, *249*, 201.
- (32) Roling, B. *J. Non-Cryst. Solids* **1999**, *244*, 34.
- (33) Di Noto, V.; Barreca, D.; Furlan, C.; Armelao, L. *Polym. Adv. Technol.* **2000**, *11*, 1.
- (34) Di Noto, V.; Vittadello, M.; Lavina, S.; Fauri, M.; Biscazzo, S. *J. Phys. Chem. B* **2001**, *105*, 4584.
- (35) Jonscher, A. K. *Dielectric Relaxations in Solids*; Chelsea Dielectrics: London, 1983.
- (36) Funke, K. Z. *Phys. Chem.* **1995**, *188*, 243.
- (37) Raistrick, I. D.; MacDonald, J. R.; Franceschetti, D. R. In *Impedance Spectroscopy*; MacDonald, J. R., Ed.; J. Wiley & Sons: New York, 1987.
- (38) Di Noto, V.; Lavina, S.; Longo, D.; Vidali, M. *Electrochim. Acta* **1998**, *43*, 1225.
- (39) Biscazzo, S.; Vittadello, M.; Lavina, S.; Di Noto, V. *Solid State Ionics* **2002**, *147*, 397.
- (40) Di Noto, V.; Münchow, V.; Vittadello, M.; Collet, J. C.; Lavina, S. *Solid State Ionics* **2002**, *147*, 397.
- (41) Boukamp, B. A. *Equivalent Circuit (EQUIVCR.T. PAS)*; Department of Chemical Technology, University of Twente: Enschede, The Netherlands 1989.
- (42) Vittadello, M.; Biscazzo, S.; Lavina, S.; Fauri, M.; Di Noto, V. *Solid State Ionics* **2002**, *147*, 341.
- (43) MacDonald, J. R.; Johnson, W. B. In *Impedance Spectroscopy*; MacDonald, J. R., Ed.; J. Wiley & Sons: New York, 1987; p 23.
- (44) Funke, K. *Ber. Bunsen-Ges. Phys. Chem.* **1991**, *95*, 955.
- (45) Cramer, C.; Funke, K.; Seatkamp, T.; Wilmer, D.; Ingram, M. D. *Naturforsch. A* **1995**, *50*, 613.
- (46) Bunde, A.; Ingram, M. D.; Maass, P. *J. Non-Cryst. Solids* **1994**, *172*, 1222.
- (47) Ward, I. M.; Boden, N.; Cruickshank, J.; Leng, S. A. *Electrochim. Acta* **1995**, *40*, 2071.
- (48) Latham, R. J.; Linford, R. G. *Solid State Ionics* **1996**, *85*, 193.
- (49) Frech, R.; Chintapalli, S.; Bruce, P. G.; Vincent, C. A. *J. Chem. Soc., Chem. Commun.* **1997**, 157.
- (50) Shi, J.; Vincent, C. A. *Solid State Ionics* **1993**, *60*, 11.
- (51) Fox, T. G. *Bull. Am. Phys. Soc.* **1956**, *1*, 123.
- (52) Sun, J.; MacFarlane, D. R.; Forsyth, M. *J. Polym. Sci. A Polym. Chem.* **1996**, *34*, 3465.
- (53) Bishop, A. G.; MacFarlane, R. D.; Forsyth, M. *Electrochim. Acta* **1998**, *43*, 1453.
- (54) Bockris, J. O'M.; Reddy, A. K. N. *Modern Electrochemistry*, Plenum-Rosetta: New York, 1977; Vol. 1, Chapter 4.
- (55) Ferry, A.; Jacobsson, P.; Torell, L. M. *Electrochim. Acta* **1995**, *40*, 2369.